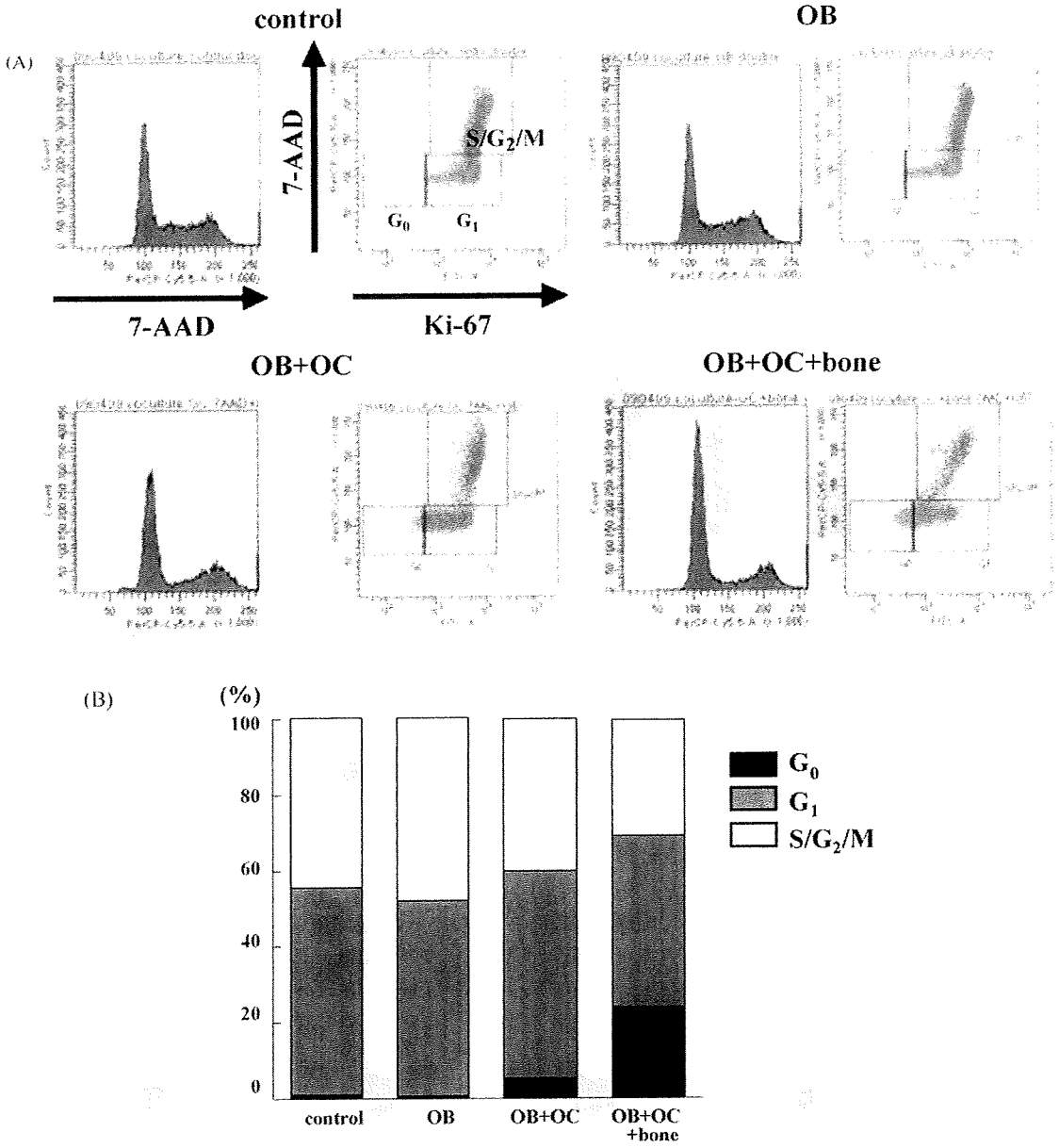

Fig. 2. OCs with bone slices increased the Ki-67-negative G_0 population in Ba/F3 wt *bcr-abl* cells. (A) Each figure shows representative data from three independent experiments. Co-cultured Ba/F3 wt *bcr-abl* cells were harvested 72 h after co-culture was initiated and were analyzed for their cell cycle status by flow cytometry following 7-AAD and Ki-67 staining. The percentages of cells in each cell cycle phase are shown in (B).

which confirms that the bone slices themselves did not influence the growth of Ba/F3 wt *bcr-abl* cells (Fig. 1B). Mature OCs identified by TRAP staining were observed in wells with OB + OC and OB + OC + bone, indicating that mature OCs were maintained in these co-culture experiments. In OB + OC + bone wells, $TRAP^+$ OCs were also observed on the bone slices (Fig. 1C).

3.2. OCs induced Ki-67-negative population in leukemic cells

We next sought to determine the source of growth suppression of Ba/F3 wt *bcr-abl* cells in the OB + OC + bone co-culture. First, we examined the cell cycle status of Ba/F3 wt *bcr-abl* cells co-cultured with OBs, OCs and/or bone slices. Ki-67 is expressed throughout all the cell cycle phases except G_0, thus 7-AAD and Ki-67 staining can distinguish cells in G_0 from those in G_0/G_1 by flow cytometry [17]. Interestingly, compared to the OB + OC co-culture, cells in the OB + OC + bone co-culture had an obviously increased Ki-67-negative population, which indicates resting cells in G_0 phase (Fig. 2A and B).

3.3. Effect of TGF-β_1 released or produced in the presence of bone slices on the growth of leukemic cells

Recently, TGF-β_1 was reported to be important for the maintenance of HSCs in the quiescent state in the BM niche [18]. TGF-β is also one of the major cytokines that accumulate in the bone matrix [19–21]. We speculated that OCs might suppress the growth of leukemic cells through the production or release of TGF-β_1 from the bone slices in our co-culture experiments. Thus, we used ELISA to measure the levels of TGF-β_1 in the culture supernatants. TGF-β_1 was significantly higher in supernatants from the OB + OC + bone co-culture than in supernatants from OB or OB + OC co-cultures (Fig. 3A), which suggests that OCs facilitate the release of TGF-β_1 from the bone slices. Next, we added an anti-TGF-β antibody

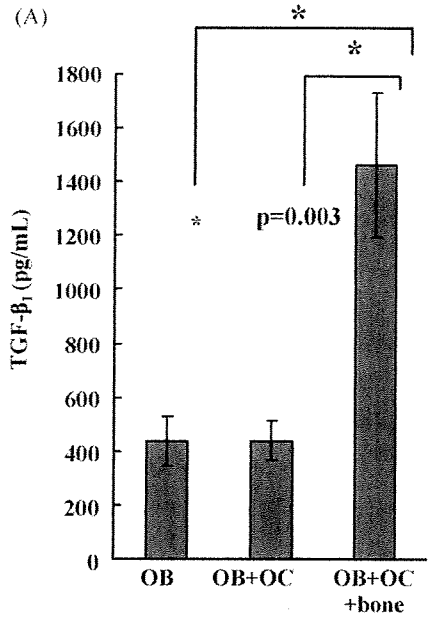

(C)

	G_0	G_1	$S/G_2/M$
control	1.0	50.5	47.7
Ab	0.6	52.8	45.7
OB	0.7	55.0	43.6
OB+Ab	0.9	48.2	48.3
OB+OC	0.8	50.2	45.1
OB+OC+Ab	0.7	54.3	44.5
OB+OC+bone	6.8	60.7	31.7
OB+OC+bone+Ab	3.8	61.4	34.7

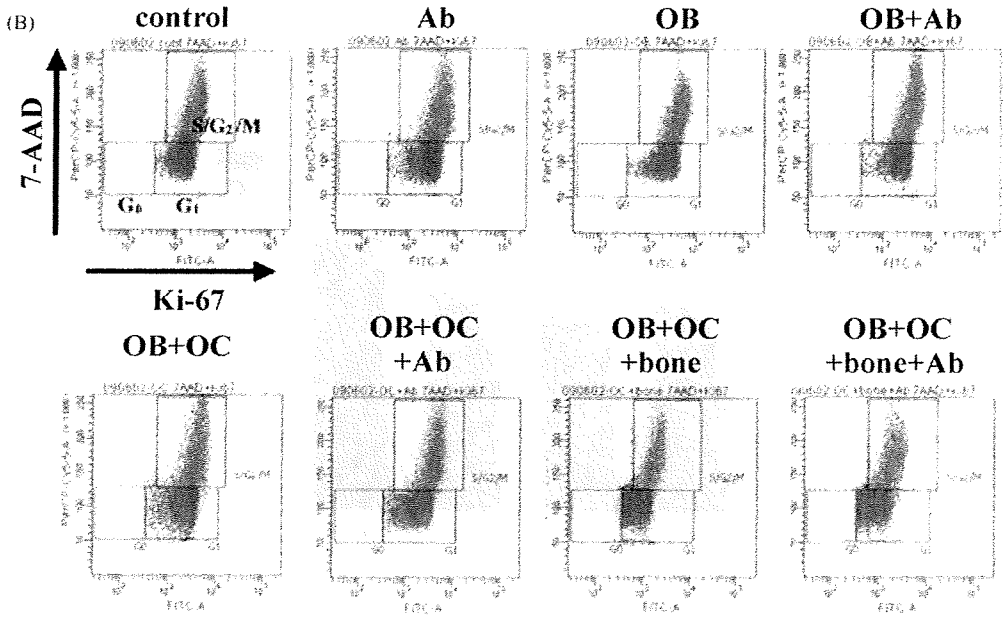

Fig. 3. TGF-β_1 released from the bone slices might affect the growth of Ba/F3 wt *bcr-abl* cells. (A) TGF-β_1 concentrations in the supernatants of OB, OB + OC, and OB + OC + bone were measured by ELISA. The results shown are the means ± SD of three independent experiments in duplicate. (B and C) 1 μg/mL of anti-TGF-β antibody was added to each co-culture condition. Cell cycle status of Ba/F3 wt *bcr-abl* cells after 72 h of co-culture was analyzed by flow cytometry following Ki-67 and 7-AAD staining. Representative results of three independent experiments are shown.

to the transwells. Addition of the anti-TGF-β antibody reduced the Ki-67-negative G_0 population in OB + OC + bone cells (Fig. 3B). These results suggest that the growth suppressive effect observed in the OB + OC + bone co-culture might be yielded, in part, via TGF-β_1.

Finally, we examined whether exogenous TGF-β_1 could increase the Ki-67-negative G_0 population in Ba/F3 wt *bcr-abl* cells. We treated Ba/F3 wt *bcr-abl* cells with various concentrations of recombinant TGF-β_1 and/or anti-TGF-β antibody. TGF-β_1 suppressed the growth of Ba/F3 wt *bcr-abl* cells and slightly increased the Ki-67-negative population, while the addition of the anti-TGF-β antibody completely suppressed this effect (Fig. 4A–C). We confirmed that the TGF-β antibody inhibited the phosphorylation of Smad2, a major signaling molecule of the TGF-β pathway (Fig. 4D). Therefore, it appears that the TGF-β antibody might reduce the dormant Ki-67-negative Ba/F3 population in the co-culture experiments through inhibition of the TGF-β pathway.

4. Discussion

Leukemic cells have been suggested to interact closely with the BM microenvironment [22]. It is believed that in this environment they receive various signals that are able to protect the leukemic cells from apoptosis induced by anti-cancer drugs and promote their survival or proliferation [23–27]. The BM microenvironment has also been implicated in the induction of myeloproliferative syn-

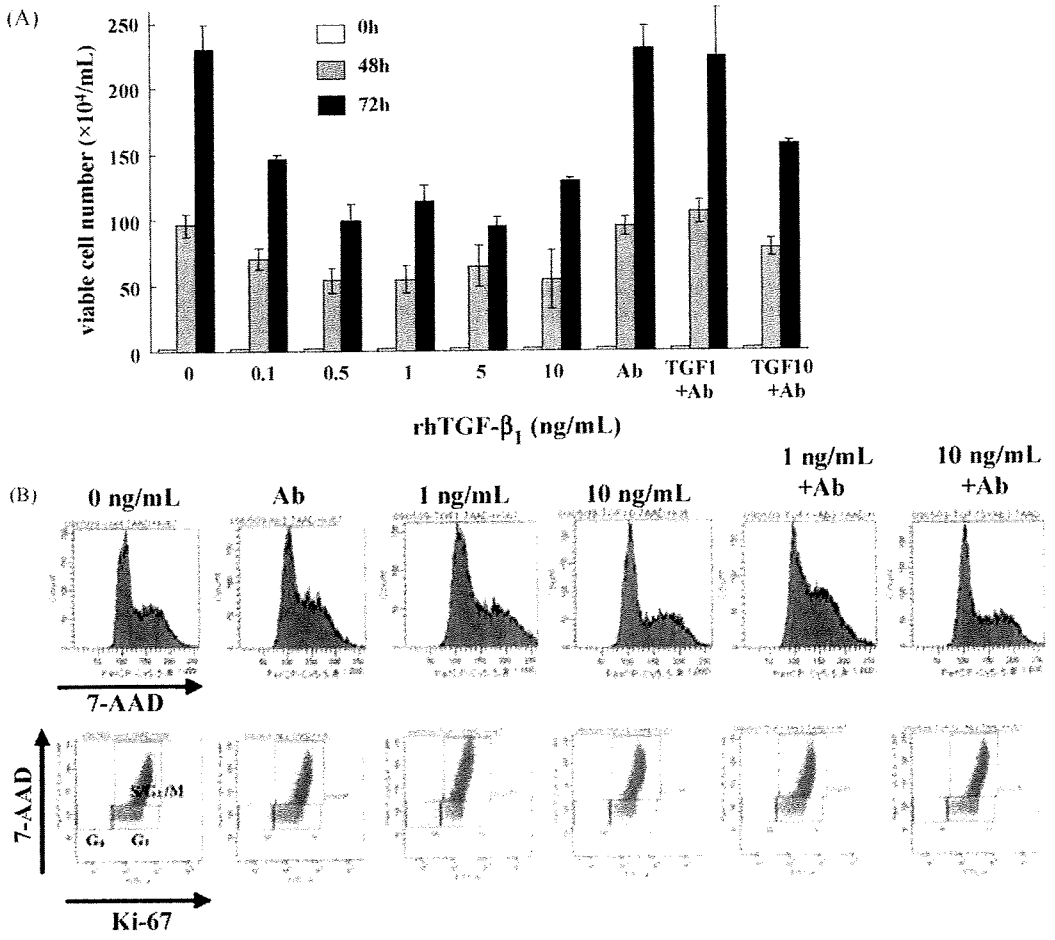

TGF-β1 (ng/mL)	G_0	G_1	$S/G_2/M$
0	1.2	49.2	50.3
1	2.2	42.3	56.3
10	1.5	50.6	48.4
Ab	2.3	46.7	51.4
1+Ab	0.8	42.4	57.6
10+Ab	1.0	50.0	49.5

Fig. 4. TGF-β_1 might maintain Ba/F3 wt *bcr-abl* cells in a dormant state. (A) Ba/F3 wt *bcr-abl* cells were treated with the indicated doses of TGF-β_1 for 72 h. The number of viable cells was counted by trypan blue staining, and (B) cell cycle analysis was performed by flow cytometry following 7-AAD and Ki-67 staining. The percentage of cells in each cell cycle phase is shown in (C). (D) Western blot analysis shows that recombinant TGF-β_1 induced phosphorylation of Smad protein, and addition of TGF-β antibody inhibited this phosphorylation in Ba/F3 wt *bcr-abl* cells.

drome through interaction with hematopoietic cells [28,29], and it was reported that leukemic cells influence the BM niche and disrupt normal hematopoiesis [30]. Recently, OCs have been shown to play a role in the mobilization of hematopoietic progenitor cells through matrix metalloproteinase-9 or cathepsin-K mediated cleavage of stromal cell-derived factor-1 (SDF-1) or stem cell factor (SCF), which anchor HSCs to the BM niche [10]. In this study, we hypothesized that the anti-tumor activity of ZOL observed in previous studies was due to a reduction in the number of mature OCs in the BM microenvironment. In cases of breast cancer [31] or prostate cancer [32] that metastasize to the bones, or in multiple myeloma [33], the close interaction between OCs and tumor cells is believed to be important for tumor progression or survival in the local microenvironment. The tumor cells activate OCs and induce bone-resorption activity, thereby increasing the available growth area and stimulating the release of growth factors from the bone matrix. Thus, it is possible that the survival or proliferation of leukemic cells is enhanced by the activity of OCs in the BM microenvironment.

Recently, it was reported that TGF-β might induce HSC hibernation in the BM niche [18]. TGF-β signaling plays an important role in the regulation of normal hematopoiesis by preventing progression through the cell cycle and promoting differentiation [34–36]. In acute myelogenous leukemia (AML) or CML, impairment of the negative growth-regulatory effects exerted by TGF-β signaling has been reported to contribute to the transformation, persistence, and maintenance of leukemic clones, and also to the development of drug resistance in leukemic cells [37–39].

In our co-culture experiments, OCs were able to increase the population of Ki-67-negative dormant leukemic cells only in the

presence of bone slices, and higher levels of TGF-β_1 were detected in the supernatants of cells in the OB + OC + bone co-culture. Therefore, it appears that OCs might maintain leukemic cells in a quiescent state in the BM microenvironment through the release of TGF-β. Quiescence is also likely to be important for the survival of leukemia-initiating cells (LICs) or leukemia stem cells (LSCs) [40,41]. Thus, these quiescent cells in the BM niche could become effective targets for the treatment of leukemia [42]. Our data suggests that TGF-β released or produced in the BM niche by OCs might contribute to the maintenance of quiescent LIC or LSC populations.

However, it remains unclear why OB + OC + bone could increase the Ki-67-negative G_0 population more strongly than recombinant TGF-β_1. One possible explanation is that other cytokines produced or released in OB + OC + bone co-culture in addition to TGF-β_1 regulate the proliferation of leukemic cells and work synergistically with TGF-β_1. Another possibility is that TGF-β_1 might induce the production of other soluble factors that affect the cell cycle progression of leukemic cells by OCs. Further experiments are necessary to better define the mechanism by which OCs and TGF-β_1 are able to influence the growth of leukemic cells.

5. Conclusion

In conclusion, our data indicates that OCs might represent a novel target for the development of therapies that target dormant leukemic cells in the BM microenvironment, thereby potentially reducing the incidence of relapse and the onset of acquired drug resistance in leukemic diseases.

Conflict of interest statement

The authors report no potential conflicts of interest.

Acknowledgements

We gratefully thank Prof. Naoyuki Takahashi and Prof. Nobuyuki Udagawa, Matsumoto Dental University, for technical advice, and Yoko Nakagawa for her excellent technical support. This work was supported by a Grant-in-Aid for Japan Society for the Promotion of Science (JSPS) Fellows.

Contributions. Asumi Yokota, Shinya Kimura, Eishi Ashihara and Taira Maekawa designed research; Asumi Yokota, Ruriko Tanaka, Miki Takeuchi, Yao Hisayuki, Kazuki Sakai, Rina Nagao, Junya Kuroda, Yuri Kamitsuji, Eri Kawata and Eishi Ashihara performed research; Asumi Yokota and Shinya Kimura analyzed data; Asumi Yokota, Shinya Kimura and Taira Maekawa wrote the paper.

References

[1] Calvi LM, Adams GB, Weibrecht KW, Weber JM, Olson DP, Knight MC, et al. Osteoblastic cells regulate the haematopoietic stem cell niche. Nature 2003;425:841–6.
[2] Zhang J, Niu C, Ye L, Huang H, He X, Tong WG, et al. Identification of the haematopoietic stem cell niche and control of the niche size. Nature 2003;425:836–41.
[3] Arai F, Hirao A, Ohmura M, Sato H, Matsuoka S, Takubo K, et al. Tie2/angiopoietin-1 signaling regulates hematopoietic stem cell quiescence in the bone marrow niche. Cell 2004;118:149–61.
[4] Yoshihara H, Arai F, Hosokawa K, Hagiwara T, Takubo K, Nakamura Y, et al. Thrombopoietin/MPL signaling regulates hematopoietic stem cell quiescence and interaction with the osteoblastic niche. Cell Stem Cell 2007;1:685–97.
[5] Hosokawa K, Arai F, Yoshihara H, Nakamura Y, Gomei Y, Iwasaki H, et al. Function of oxidative stress in the regulation of hematopoietic stem cell–niche interaction. Biochem Biophys Res Commun 2007;363:578–83.
[6] Kubota Y, Takubo K, Suda T. Bone marrow long label-retaining cells reside in the sinusoidal hypoxic niche. Biochem Biophys Res Commun 2008;366:335–9.
[7] Takahashi N, Akatsu T, Udagawa N, Sasaki T, Yamaguchi A, Moseley JM, et al. Osteoblastic cells are involved in osteoclast formation. Endocrinology 1988;123:2600–2.
[8] Lacey DL, Timms E, Tan HL, Kelley MJ, Dunstan CR, Burgess T, et al. Osteoprotegerin ligand is a cytokine that regulates osteoclast differentiation and activation. Cell 1998;93:165–76.
[9] Boyle WJ, Simonet WS, Lacey DL. Osteoclast differentiation and activation. Nature 2003;423:337–42.
[10] Kollet O, Dar A, Shivtiel S, Kalinkovich A, Lapid K, Sztainberg Y, et al. Osteoclasts degrade endosteal components and promote mobilization of hematopoietic progenitor cells. Nat Med 2006;12:657–64.
[11] Shivtiel S, Kollet O, Lapid K, Schajnovitz A, Goichberg P, Kalinkovich A, et al. CD45 regulates retention, motility, and numbers of hematopoietic progenitors, and affects osteoclast remodeling of metaphyseal trabecules. J Exp Med 2008;205:2381–95.
[12] Adams GB, Chabner KT, Alley IR, Olson DP, Szczepiorkowski ZM, Poznansky MC, et al. Stem cell engraftment at the endosteal niche is specified by the calcium-sensing receptor. Nature 2006;439:599–603.
[13] Kuroda J, Kimura S, Segawa H, Kobayashi Y, Yoshikawa T, Urasaki Y, et al. The third-generation bisphosphonate zoledronate synergistically augments the anti-Ph+ leukemia activity of imatinib mesylate. Blood 2003;102:2229–35.
[14] Kimura S, Kuroda J, Segawa H, Sato K, Nogawa M, Yuasa T, et al. Antiproliferative efficacy of the third-generation bisphosphonate, zoledronic acid, combined with other anticancer drugs in leukemic cell lines. Int J Hematol 2004;79:37–43.
[15] Segawa H, Kimura S, Kuroda J, Sato K, Yokota A, Kawata E, et al. Zoledronate synergises with imatinib mesylate to inhibit Ph primary leukaemic cell growth. Br J Haematol 2005;130:558–60.
[16] Kimura S, Naito H, Segawa H, Kuroda J, Yuasa T, Sato K, et al. NS-187, a potent and selective dual Bcr-Abl/Lyn tyrosine kinase inhibitor, is a novel agent for imatinib-resistant leukemia. Blood 2005;106:3948–54.
[17] van Pelt K, de Haan G, Vellenga E, Daenen SM. Administration of low-dose cytarabine results in immediate S-phase arrest and subsequent activation of cell cycling in murine stem cells. Exp Hematol 2005;33:226–31.
[18] Yamazaki S, Iwama A, Takayanagi S, Eto K, Ema H, Nakauchi H. TGF-beta as a candidate bone marrow niche signal to induce hematopoietic stem cell hibernation. Blood 2009;113:1250–6.
[19] Seyedin SM, Thomas TC, Thompson AY, Rosen DM, Piez KA. Purification and characterization of two cartilage-inducing factors from bovine demineralized bone. Proc Natl Acad Sci USA 1985;82:2267–71.
[20] Centrella M, Canalis E. Transforming and nontransforming growth factors are present in medium conditioned by fetal rat calvariae. Proc Natl Acad Sci USA 1985;82:7335–9.
[21] Seyedin SM, Thompson AY, Bentz H, Rosen DM, McPherson JM, Conti A, et al. Cartilage-inducing factor-A. Apparent identity to transforming growth factor-beta. J Biol Chem 1986;261:5693–5.
[22] Lane SW, Scadden DT, Gilliland DG. The leukemic stem cell niche—current concepts and therapeutic opportunities. Blood 2009.
[23] Matsunaga T, Takemoto N, Sato T, Takimoto R, Tanaka I, Fujimi A, et al. Interaction between leukemic-cell VLA-4 and stromal fibronectin is a decisive factor for minimal residual disease of acute myelogenous leukemia. Nat Med 2003;9:1158–65.
[24] Ishikawa F, Yoshida S, Saito Y, Hijikata A, Kitamura H, Tanaka S, et al. Chemotherapy-resistant human AML stem cells home to and engraft within the bone-marrow endosteal region. Nat Biotechnol 2007;25:1315–21.
[25] Ninomiya M, Abe A, Katsumi A, Xu J, Ito M, Arai F, et al. Homing, proliferation and survival sites of human leukemia cells in vivo in immunodeficient mice. Leukemia 2007;21:136–42.
[26] Fleming HE, Janzen V, Lo Celso C, Guo J, Leahy KM, Kronenberg HM, et al. Wnt signaling in the niche enforces hematopoietic stem cell quiescence and is necessary to preserve self-renewal in vivo. Cell Stem Cell 2008;2:274–83.
[27] Jin L, Tabe Y, Konoplev S, Xu Y, Leysath CE, Lu H, et al. CXCR4 up-regulation by imatinib induces chronic myelogenous leukemia (CML) cell migration to bone marrow stroma and promotes survival of quiescent CML cells. Mol Cancer Ther 2008;7:48–58.
[28] Walkley CR, Olsen GH, Dworkin S, Fabb SA, Swann J, McArthur GA, et al. A microenvironment-induced myeloproliferative syndrome caused by retinoic acid receptor gamma deficiency. Cell 2007;129:1097–110.
[29] Walkley CR, Shea JM, Sims NA, Purton LE, Orkin SH. Rb regulates interactions between hematopoietic stem cells and their bone marrow microenvironment. Cell 2007;129:1081–95.
[30] Colmone A, Amorim M, Pontier AL, Wang S, Jablonski E, Sipkins DA. Leukemic cells create bone marrow niches that disrupt the behavior of normal hematopoietic progenitor cells. Science 2008;322:1861–5.
[31] Cicek M, Oursler MJ. Breast cancer bone metastasis and current small therapeutics. Cancer Metastasis Rev 2006;25:635–44.
[32] Bradley DA, Hussain M, Dipaola RS, Kantoff P. Bone directed therapies for prostate cancer. J Urol 2007;178:S42–8.
[33] Silvestris F, Lombardi L, De Matteo M, Bruno A, Dammacco F. Myeloma bone disease: pathogenetic mechanisms and clinical assessment. Leuk Res 2007;31:129–38.
[34] Chadwick K, Shojaei F, Gallacher L, Bhatia M. Smad7 alters cell fate decisions of human hematopoietic repopulating cells. Blood 2005;105:1905–15.
[35] Larsson J, Karlsson S. The role of Smad signaling in hematopoiesis. Oncogene 2005;24:5676–92.
[36] Chabanon A, Desterke C, Rodenburger E, Clay D, Guerton B, Boutin L, et al. A cross-talk between stromal cell-derived factor-1 and transforming growth factor-beta controls the quiescence/cycling switch of CD34(+) progenitors through FoxO3 and mammalian target of rapamycin. Stem Cells 2008;26:3150–61.

[37] Atfi A, Abecassis L, Bourgeade MF. Bcr-Abl activates the AKT/Fox O3 signalling pathway to restrict transforming growth factor-beta-mediated cytostatic signals. EMBO Rep 2005;6:985–91.
[38] Dong M, Blobe GC. Role of transforming growth factor-beta in hematologic malignancies. Blood 2006;107:4589–96.
[39] Moller GM, Frost V, Melo JV, Chantry A. Upregulation of the TGFbeta signalling pathway by Bcr-Abl: implications for haemopoietic cell growth and chronic myeloid leukaemia. FEBS Lett 2007;581:1329–34.
[40] Jordan CT, Guzman ML. Mechanisms controlling pathogenesis and survival of leukemic stem cells. Oncogene 2004;23:7178–87.
[41] Ito K, Bernardi R, Morotti A, Matsuoka S, Saglio G, Ikeda Y, et al. PML targeting eradicates quiescent leukaemia-initiating cells. Nature 2008;453:1072–8.
[42] Elrick LJ, Jorgensen HG, Mountford JC, Holyoake TL. Punish the parent not the progeny. Blood 2005;105:1862–6.

ARTICLE IN PRESS

Cancer Letters xxx (2010) xxx–xxx

Contents lists available at ScienceDirect

Cancer Letters

journal homepage: www.elsevier.com/locate/canlet

A combination of a DNA-chimera siRNA against PLK-1 and zoledronic acid suppresses the growth of malignant mesothelioma cells *in vitro*

Eri Kawata [a,b,1], Eishi Ashihara [a,*,1], Yoko Nakagawa [a], Takahiro Kiuchi [a], Mai Ogura [a], Hisayuku Yao [a], Kazuki Sakai [a], Ruriko Tanaka [a], Rina Nagao [a], Asumi Yokota [a], Miki Takeuchi [a], Shinya Kimura [c], Hideyo Hirai [a], Taira Maekawa [a]

[a] *Department of Transfusion Medicine & Cell Therapy, Kyoto University Hospital, 54 Kawahara-cho Shogoin, Sakyo-ku, Kyoto 606-8507, Japan*
[b] *Division of Internal Medicine, Kyoto Second Red Cross Hospital, 355 Kamannza Marutamachi, Kamigyo-ku, Kyoto 602-8026, Japan*
[c] *Division of Hematology, Respiratory Medicine, and Oncology, Department of Internal Medicine, Faculty of Medicine, Saga University, 5-1-1 Nabeshima, Saga 849-8501, Japan*

ARTICLE INFO

Article history:
Received 24 November 2009
Received in revised form 6 February 2010
Accepted 10 February 2010
Available online xxxx

Keywords:
PLK-1
RNA interference
DNA-chimeric siRNA
Bisphosphonate
Malignant mesothelioma

ABSTRACT

Although novel agents effective against malignant mesothelioma (MM) have been developed, the prognosis of patients with MM is still poor. We generated a DNA-chimeric siRNA against polo-like kinase-1 (PLK-1), which was more stable in human serum than the non-chimeric siRNA. The chimeric PLK-1 siRNA inhibited MM cell proliferation through the induction of apoptosis. Next, we investigated the effects of zoledronic acid (ZOL) on MM cells, and found that ZOL also induced apoptosis in MM cells. Furthermore, ZOL augmented the inhibitory effects of the PLK-1 siRNA. In conclusion, combining a PLK-1 siRNA with ZOL treatment is an attractive strategy against MM.

1. Introduction

Malignant mesothelioma (MM) is an aggressive tumor, which develops from the mesothelial surface of the pleural and peritoneal cavities. Asbestos is well-known as a carcinogen in MM and the incidence of MM is increasing worldwide [1]. Although several surgical approaches have been proven to be effective [2,3], a combination of therapies including chemotherapeutic agents, radiation, and immunotherapy are required to fight the disease. However, in spite of the emergence of novel effective anticancer agents such as pemetrexed [4,5] and raltitrexed [6,7], the prognosis of patients with MM is still poor [8,9]. Therefore, the development of novel effective therapeutic strategies is essential to improve the prognosis of this disease.

RNA interference (RNAi) is a process involving sequence specific post-transcriptional gene silencing induced by double-stranded (ds) RNA. It is widely applied as a powerful tool in postgenomic research, and has been experimentally introduced into the field of cancer therapy. Synthetic, short interfering RNAs (siRNAs) for inducing RNAi are 19- to 21-nucleotide dsRNAs with two-nucleotide 3′ overhangs at either end [10,11]. Unfotunately, siRNAs are degraded by endogenous nucleases when administered *in vivo*. Many techniques, including the use of DNA-chimeric siRNAs, have been developed to protect siRNAs from such degradation [10,12,13]. Previous investigations have revealed that their silencing activity is as powerful as that of non-chimeric siRNAs [12–14].

Polo-like kinase-1 (PLK-1) belongs to the PLK family of serine/threonine kinases and is highly conserved among eukaryotes. PLK-1 regulates cell division at several points during the mitotic phase of the cell cycle, including: mitotic entry through CDK1 activation, bipolar spindle

* Corresponding author. Tel.: +81 75 751 3630; fax: +81 75 751 4283.
E-mail address: ash0325@kuhp.kyoto-u.ac.jp (E. Ashihara).
[1] These authors contribute equal to this work.

0304-3835/$ - see front matter © 2010 Elsevier Ireland Ltd. All rights reserved.
doi:10.1016/j.canlet.2010.02.008

Please cite this article in press as: E. Kawata et al., A combination of a DNA-chimera siRNA against PLK-1 and zoledronic acid suppresses the growth of malignant mesothelioma cells *in vitro*, Cancer Lett. (2010), doi:10.1016/j.canlet.2010.02.008

formation, chromosome alignment, segregation of chromosomes, and cytokinesis [15,16]. Previous studies have reported that PLK-1 is overexpressed in cancerous tissues and that PLK-1 expression levels are tightly correlated with histological grades of tumors, clinical stages, and the patients' prognosis [17–20]. Thus, PLK-1 is considered to be a suitable target for cancer therapy, and several small molecular targeting agents have been used in clinical trials [21,22], while siRNAs against PLK-1 have been investigated in preclinical studies [19,20,23].

Bisphosphonates (BPs) are inhibitors of bone-resorption, and second- and third-generation BPs have been developed primarily to treat benign and malignant bone disease [24]. This class of drugs inhibits the proliferation of cancer cells by preventing the post-translational prenylation of small GTPases including the Ras family proteins [25]. We have demonstrated previously that third-generation BPs such as zoledronic acid (ZOL) and minodronic acid (YM529) have direct anti-tumor effects against different cancer cells [26–30].

In the present study, we have investigated the effects of a DNA-chimeric PLK-1 siRNA and ZOL on MM cells *in vitro*. Our results show that these agents induce apoptosis and inhibit the proliferation of MM cells. In addition, we found that ZOL enhances the inhibitory effects of the PLK-1 siRNA.

2. Materials and methods

2.1. Cell lines, reagents, and animals

The human MM cell lines H2452, H2052, H28, and 211H were cultured in RPMI1640 medium (Gibco, Tokyo, Japan) containing 10% heat-inactivated fetal calf serum (FCS; Invitrogen, Tokyo, Japan), *l*-glutamine (Gibco), and 1% penicillin–streptomycin (Gibco). The normal human dermal fibroblast (NHDF) cells were cultured in Dulbecco's Modified Eagle medium (DMEM; Gibco) containing 10% FCS, *l*-glutamine, and 1% penicillin–streptomycin. All cell lines were maintained at 37 °C in a fully humidified atmosphere of 5% CO_2 in air. All four MM cell lines were obtained from the American Type Culture Collection (Rockville, MD). Normal fibroblast NHDF cells were purchased from Kurabo (Osaka, Japan). LIC™ Transfection Reagent (Hayashi Kasei, Tokyo, Japan) was used for transfection into MM cells. ZOL (1-hydroxy-2-[1*H*-imidazole-1-yl]ethylidene-bisphosphonic acid) was obtained from Novalits Pharma AG (Basel, Switzerland).

We generated two types of siRNA against PLK-1 (GenBank accession number NM_005030) using siDIRECT™ (alphaGEN Co, Ltd, Tokyo, Japan). One of the siRNAs contained of ribonucleotides and the other was a DNA-chimeric siRNA consisting partially of deoxyribonucleotides. The oligonucleotide sequences of the non-chimeric PLK-1 siRNA against PLK-1 were: sense strands, 5′- GCACCGAAACCG AGUUAUUCA-3′ and that antisense strand, 5′-AAUAACUC GGUUUCGGUGCAG-3′. The sequences of the DNA-chimeric siRNA against PLK-1 were: sense strand, 5′-GCACCGAAAC CGAgttattca-3′, and antisense strand, 5′-aataacUCGGUUU CGGUGCAG-3′. This DNA-modified siRNA was constructed by substituting six ribonucleotides at the 5′ end of the guide strand and the 3′ end of the passenger strand with the cognate deoxyribonucleotides (designated in lower case). The oligonucleotide sequences for the chimeric siRNA controls were: sense strand, 5′-GUACCGCACGUCAttcgtatt-3′, and antisense strand, 5′- tacgaaUGACGUGCG GUACGU-3′. The sequences for the non-chimeric control siRNA were: sense strand, 5′-GUACCGCACGUCAUUC GUAUU-3′, and antisense strand, 5′-UACGAAUGACGUGCG-GUACGU-3′. All siRNAs used were chemically synthesized (Hokkaido System Science Co. Ltd., Hokkaido, Japan).

2.2. Stability of the DNA-chimera siRNA in human serum

We investigated the stability of the DNA-chimeric and non-chimeric siRNAs in human serum. Each siRNA was incubated in human serum (95%) at 37 °C. Serum RNase was inactivated by adding SDS and proteinase K, and then digested samples were loaded onto 15% polyacrylamide gel, which was then stained using SYBR Gold (Invitrogen).

2.3. Growth inhibitory effects of PLK-1 siRNA

Cell proliferation was determined by the modified MTT assay using the Cell-Counting Kit-8 (Dojindo Laboratory, Kumamoto, Japan) as previously described [19,20]. Cells were seeded in a flat-bottomed 96-well plate (Becton Dickinson, Tokyo, Japan) at 3×10^3 cells in 100 μl of medium per well and incubated with serial dilutions of the DNA-chimeric siRNA for 72 h. The mean of four samples was calculated. Half-maximal inhibition constants (IC_{50}s) were determined with the nonlinear regression program CalcuSyn (Biosoft, Cambridge, UK).

2.4. Growth inhibitory effects of zoledronic acid

Cell proliferation was determined by the modified MTT assay using the Cell-Counting Kit-8 as mentioned above. Cells were seeded in a flat-bottomed 96-well plate (Becton Dickinson, Tokyo, Japan) at 3×10^3 cells in 100 μl of medium per well and incubated with serial dilutions of ZOL for 72 h. The mean of four samples was calculated. Half-maximal inhibition constants (IC_{50}s) were determined with the nonlinear regression program CalcuSyn. We also evaluated the combined effects of concurrent PLK-1 siRNA and ZOL treatment on H2452 and H28 mesothelioma cell lines and the analyzed data is shown by the combination index (CI). CI is a method for quantifying drug cytotoxic synergism based on the mass-action law principle derived from enzyme kinetic models. This method was developed by Chou and Talalay [31,32] which has been widely used to evaluate interactions of antineoplastic agents [33–36]. Cells were incubated for 72 h with six concentrations (0.25, 0.5, 0.75, 1.0, 1.5, or 2.0 times the IC_{50}) of each agent or both in combination using the constant ratio design followed by the modified MTT assay. We calculated the combination indexes (CIs) as reported previously [33–36], and calculated the fraction affected (Fa) at each dilution (for example, Fa of 0.25 equals 75% viable cells). This method provides a quantification of the synergism ($CI < 1$), additive effect

Please cite this article in press as: E. Kawata et al., A combination of a DNA-chimera siRNA against PLK-1 and zoledronic acid suppresses the growth of malignant mesothelioma cells *in vitro*, Cancer Lett. (2010), doi:10.1016/j.canlet.2010.02.008

(CI = 1), and antagonism (CI > 1) at different dose and effect levels [31]. Calculations of the CI were made under the assumption that the mechanisms of action of the evaluated drugs were not mutually exclusive.

2.5. Cell cycle and apoptosis analysis

Cell cycle analysis using propidium iodide (PI) was performed as previously described [20]. Apoptosis induced by each siRNA treatment or ZOL treatment was determined using the Annexin-V-FITC Apoptosis Detection Kit I (BD Pharmingen, San Jose, CA) as recommended by the manufacturer. Cells were analyzed with FACS CANTO II using Diva software (BD Bioscience).

2.6. Western blotting analysis

Following the transfection of cells with PLK-1 siRNA, or treatment with ZOL, as described above, the medium was aspirated and the cells were washed with ice-cold PBS (−). The cells were lysed with ice-cold RIPA buffer (50 mM Tris–HCl [pH 7.4], 0.25 M NaCl, 5 mM EDTA, 20 mM NaF, 1% NP-40) with PMSF (1 mM) and protease inhibitor (10 μg/ml). The cells were then scraped off the plate, and the suspension of cells in lysis buffer was transferred to a centrifuge tube, which was placed on ice for 15 min with an occasional vortex to ensure complete lysis. The cell suspension was then cleared by centrifugation at 14,000g for 30 min at 4 °C, and the supernatant (total cell lysis) was either used immediately or stored at −80 °C. The protein concentration was determined using the DC Protein Assay (Bio-Rad Laboratories, Osaka, Japan).

Immunoblotting was performed as previously described [20]. The following primary antibodies (Abs) were used: rabbit polyclonal anti-PLK-1 Ab (Upstate Biotechnology Inc., Charlottesville, VA); rabbit polyclonal anti-caspase-3 Ab; rabbit polyclonal anti-cleaved caspase-3 Ab (Cell Signaling Technology, Danvers, MA); polyclonal anti-Rap1A Ab (Santa Cruz Biotechnology, Santa Cruz, CA); mouse monoclonal anti-RhoA Ab (Santa Cruz Biotechnology); mouse monoclonal anti-Ras Ab (BD Bioscience), and rabbit polyclonal anti-actin Ab (Sigma–Aldrich, Tokyo, Japan).

3. Results

3.1. Stability of the DNA-chimera siRNA in human serum

An siRNA can be protected from RNase or nuclease cleavage by the partial substitution of ribonucleotides with deoxyribonucleotides at the 5′ end of the guide strand and the 3′ end of the passenger strand. Therefore, we first designed the PLK-1 siRNA using siDIRECT™ and then converted this siRNA into a DNA-chimeric siRNA. We incubated the DNA-chimeric, or non-chimeric siRNAs against PLK-1 in 95% human serum and investigated their degeneration. The non-chimeric siRNA degenerated in a time-dependent manner, while the DNA-chimeric siRNA did not degenerate for at least 120 min (Fig. 1A). This result shows that the chimeric siRNA is more stable in human serum than the non-chimeric siRNA.

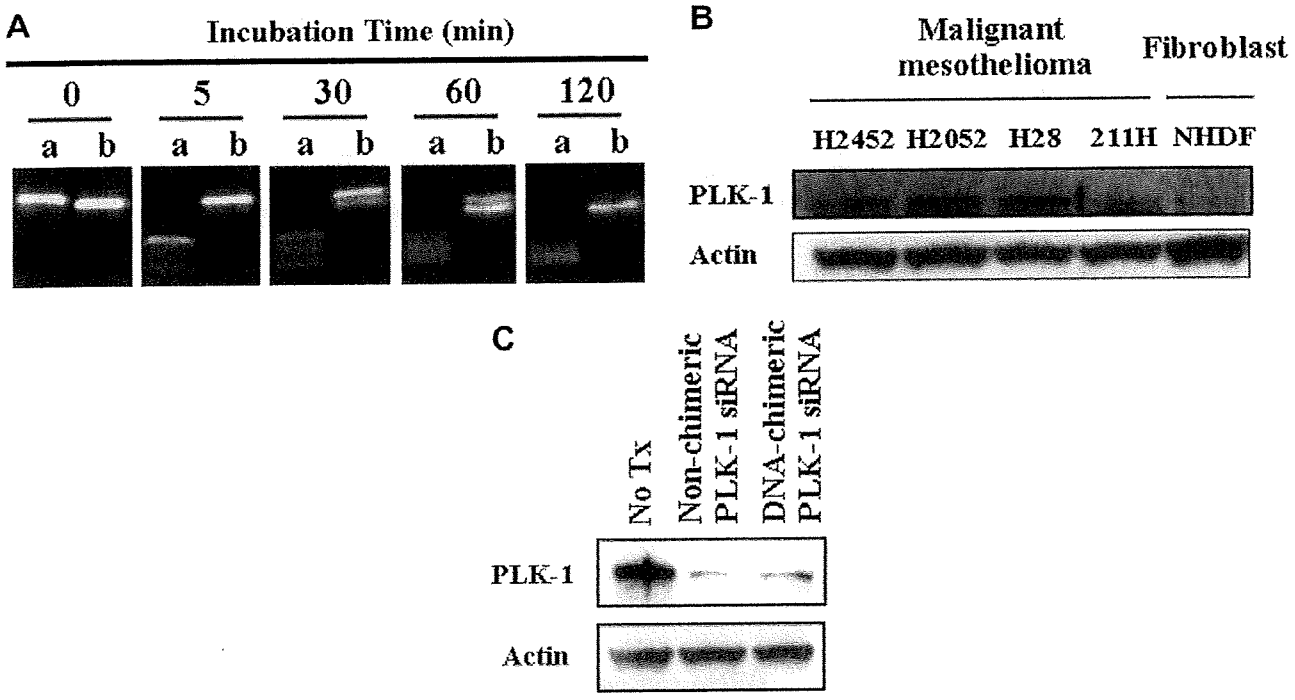

Fig. 1. DNA-chimeric siRNA against PLK-1 is more stable in human serum than a non-chimeric siRNA. (A) Each siRNA was incubated in human serum (95%) at 37 °C. Serum RNase was inactivated by adding SDS and proteinase K, and then digested samples were loaded onto a 15% polyacrylamide gel. The gel was stained by SYBR Gold. (a): non-chimeric PLK-1 siRNA, (b): DNA-chimeric PLK-1 siRNA. (B) PLK-1 expression in MM cells. Immunoblotting of whole cell lysates obtained from MM cell lines and normal NHDF human fibroblast cells. (C) Depletion of PLK-1 expression in H2452 MM cells in response to treatment with non-chimeric or DNA-chimeric PLK-1 siRNA. We obtained whole cell lysetas from H2452 MM cells 72 h after the transfection of non-chimeric or DNA-chimeric PLK-1 siRNA (50 nM), and immunoblotting was performed as described in Section 2.

Please cite this article in press as: E. Kawata et al., A combination of a DNA-chimera siRNA against PLK-1 and zoledronic acid suppresses the growth of malignant mesothelioma cells *in vitro*, Cancer Lett. (2010), doi:10.1016/j.canlet.2010.02.008

3.2. DNA-chimeric PLK-1 siRNA inhibited the growth of mesothelioma cells

We examined the PLK-1 expression in four MM cell lines: H2452, H2042, H28, and 211H cell lines. All cell lines examined expressed a higher level of PLK-1 than normal NHDF fibroblast cells (Fig. 1B). Next we confirmed the knockdown effects of both DNA-chimeric and non-chimeric PLK-1 siRNAs in MM cells. We transfected both types of siRNAs into H2452 MM cells, and both siRNAs effectively knocked down PLK-1 expression (Fig. 1C). Then we investigated the inhibitory effects of the DNA-chimeric PLK-1 siRNA on MM cells *in vitro*. Western blot analysis showed that the transfection of the DNA-chimeric PLK-1 siRNA suppressed PLK-1 expression in H2452 mesothelioma cells in a dose-dependent manner, whereas the nonsense chimeric siRNA (100 nM) did not (Fig. 2A). The IC_{50} values for H2452 and H28 cells at 72 h exposure were 1.6 nM and 38.7 nM, respectively. Out next step was to examine the growth inhibitory effects of the DNA-chimeric siRNA against PLK-1 on H2452 and H28 mesothelioma cells using a modified MTT assay. As shown in Fig. 2B, the chimeric PLK-1 siRNA inhibited cell growth in a dose-dependent manner, whereas no significant inhibitory effects were detected in normal NHDF cells (Fig. 2C).

3.3. The mechanisms of cell death induced by PLK-1 depletion

Next we investigated the mechanisms of cell death caused by PLK-1 siRNA transfection. Cell cycle analysis confirmed that PLK-1 siRNA treatment induced G2/M arrest as previously reported [19,20], and revealed an increase in the subG1 fraction 72 h after transfection with the DNA-chimeric PLK-1 siRNA (Fig. 3A, upper panel). Early apoptotic cells (Annexin – V+/PI – fraction), and late apoptotic cells and necrotic cells

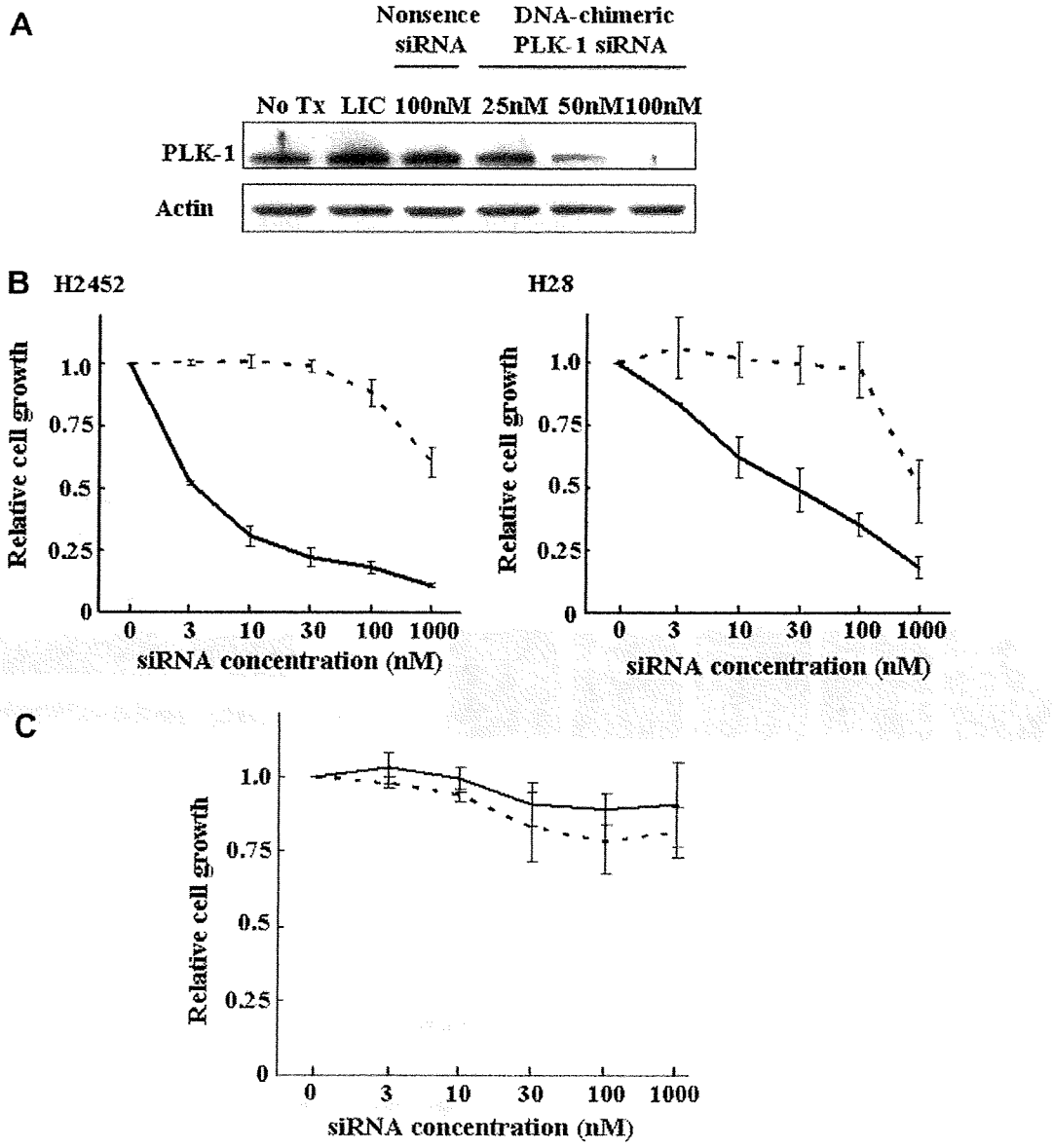

Fig. 2. DNA-chimeric PLK-1 siRNA inhibits the proliferation of MM cells, but not NHDF normal fibroblast cells. (A) Expression of PLK-1 in H2452 MM cell lines. H2452 cells were incubated with serial dilutions of DNA-chimeric PLK-1 siRNA and LIC transfection reagent for 72 h. Whole cell lysates were obtained and immunoblotting was performed as described in Section 2. (B) Cell proliferation was determined by the modified MTT assay as described in Section 2. DNA-chimeric PLK-1 siRNA shows inhibitory growth effects on H2452 and H28 MM cells in a dose-dependent manner. (C) DNA-chimeric PLK-1 siRNA does not inhibit the proliferation of normal NHDF fibroblast cells. Data represents the means ± standard deviations (SD) of three independent experiments. Solid and dotted lines indicate chimeric PLK-1 siRNA and chimeric control siRNA, respectively.

Please cite this article in press as: E. Kawata et al., A combination of a DNA-chimera siRNA against PLK-1 and zoledronic acid suppresses the growth of malignant mesothelioma cells *in vitro*, Cancer Lett. (2010), doi:10.1016/j.canlet.2010.02.008

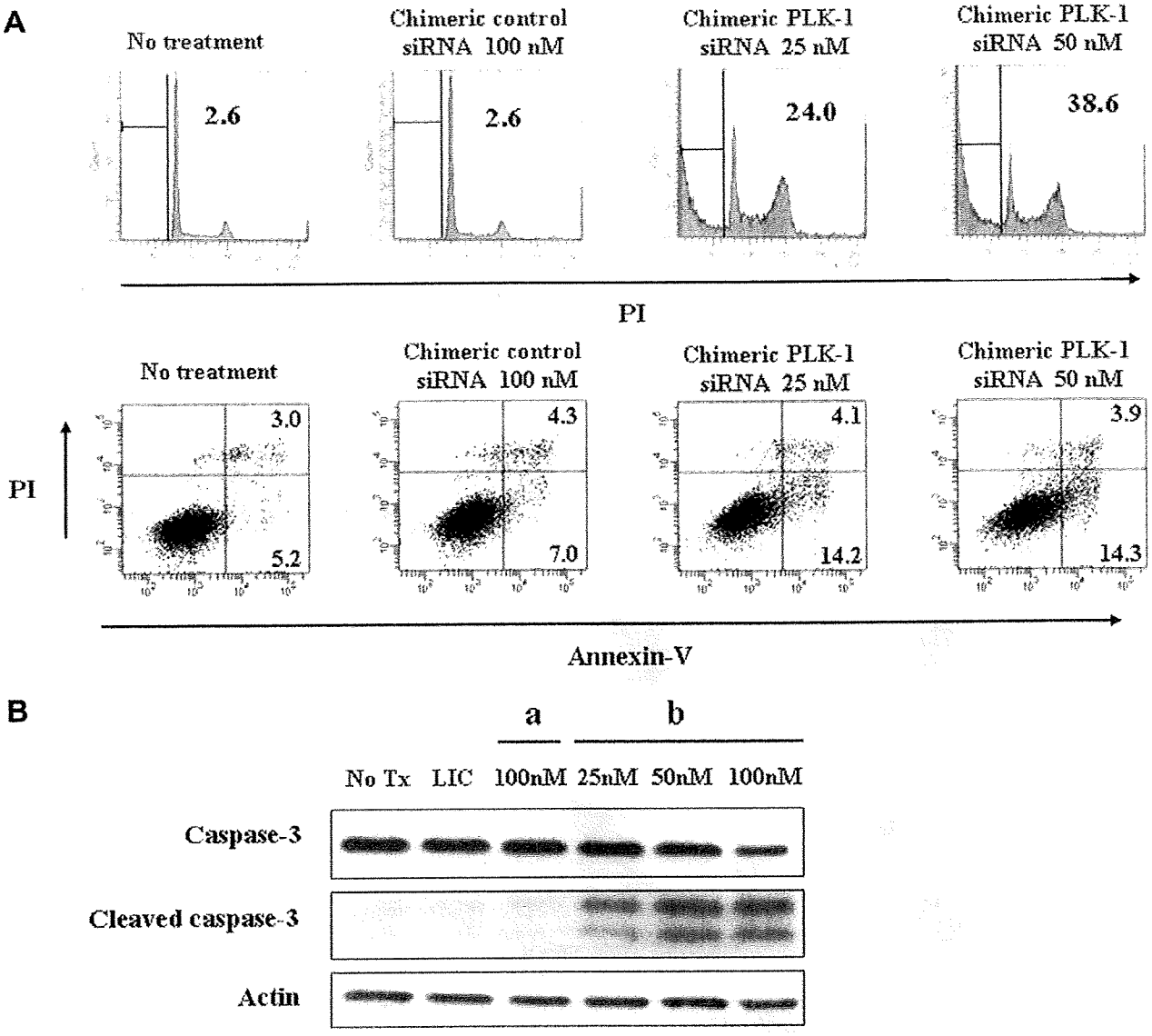

Fig. 3. DNA-chimeric PLK-1 siRNA treatment induces apoptosis in H2452 MM cells by activating caspase-3. (A: upper panels) Cell cycle analysis in H2454 MM cells using propidium iodide (PI) was performed after 72 h of treatment with the chimeric control, or chimeric PLK-1 siRNAs, at the concentration indicated. Results are representative of three independent experiments. The numbers inside each histogram indicate the percentage of the subG1 fraction. (A: lower panels) Determination of apoptosis induced by each siRNA treatment. Results are representative of three independent experiments. The numbers inside each quadrant indicate the percentage of the cell population with the quadrant characteristic. (B) Cleavage of caspase-3 by DNA-chimeric PLK-1 siRNA treatment. H2452 cells were incubated with serial dilutions of DNA-chimeric PLK-1 siRNA and LIC transfection reagent for 72 h. Whole cell lysates were obtained and immunoblotting was performed as described in Section 2. (a): chimeric control siRNA, (b): chimeric PLK-1 siRNA.

(Annexin – V+/PI + fraction) also increased after DNA-chimeric PLK-1 siRNA transfection (Fig. 3A, lower panel). In addition, Western blotting analysis demonstrated an increase in cleaved caspase-3 activity following PLK-1 siRNA transfection (Fig. 3B). Thus, transfection with a PLK-1 siRNA transfection resulted in the induction of apoptosis in mesothelioma cells through the activation of caspase-3.

3.4. ZOL inhibits the growth of mesothelioma cells and synergistically augments with the effects of the PLK-1 siRNA

We examined the inhibitory effects of ZOL on H2452 and H28 mesothelioma cells using a modified MTT assay. ZOL inhibited cell growth in a dose-dependent manner, and the IC_{50} values for H2452 and H28 cells at 72 h exposures were 11.4 μM and 58.1 μM, respectively (Fig. 4A). ZOL treatment increased the subG1 fractions (Fig. 4B) and the number of apoptotic cells (Fig. 4C) in a dose-dependent manner. Furthermore, we found that caspase-3 was cleaved by ZOL treatment (Fig. 5A).

Next we investigated the unprenylation of Rap1A, RhoA, and Ras proteins. MM cell lysates were analyzed by Western blotting using Abs against Ras and the unprenylated form of Rap1A and RhoA. ZOL treatment resulted in an increase in unprenylated Rap1A and RhoA in MM cells (Fig. 5B). The anti-Ras Ab recognizes both a slower migrating band, representing the unprenylated Ras, and a faster migrating band representing the prenylated Ras [37]. After ZOL treatment, there was an increase in the unprenylated form of Ras in MM cells which was accompanied by a reduction in the prenylated form (Fig. 5B). Taken together, the results indicate that ZOL treatment induced apoptosis through the cleavage of caspase by blocking the prenylation of small GTP-binding proteins, which resulted in the inhibition of cell growth of MM cells.

We then investigated the combined effects of ZOL treatment with the PLK-1 siRNA on H2452 and H28 MM cells. PLK-1 regulates RhoA in the mitotic phase [38,39]. The modified MTT assay with six concentrations (0.25, 0.5, 0.75, 1.0, 1.5, or 2.0 times the IC_{50}) of each agent or both in combination with the constant ratio was carried out. The values of the

Please cite this article in press as: E. Kawata et al., A combination of a DNA-chimera siRNA against PLK-1 and zoledronic acid suppresses the growth of malignant mesothelioma cells *in vitro*, Cancer Lett. (2010), doi:10.1016/j.canlet.2010.02.008

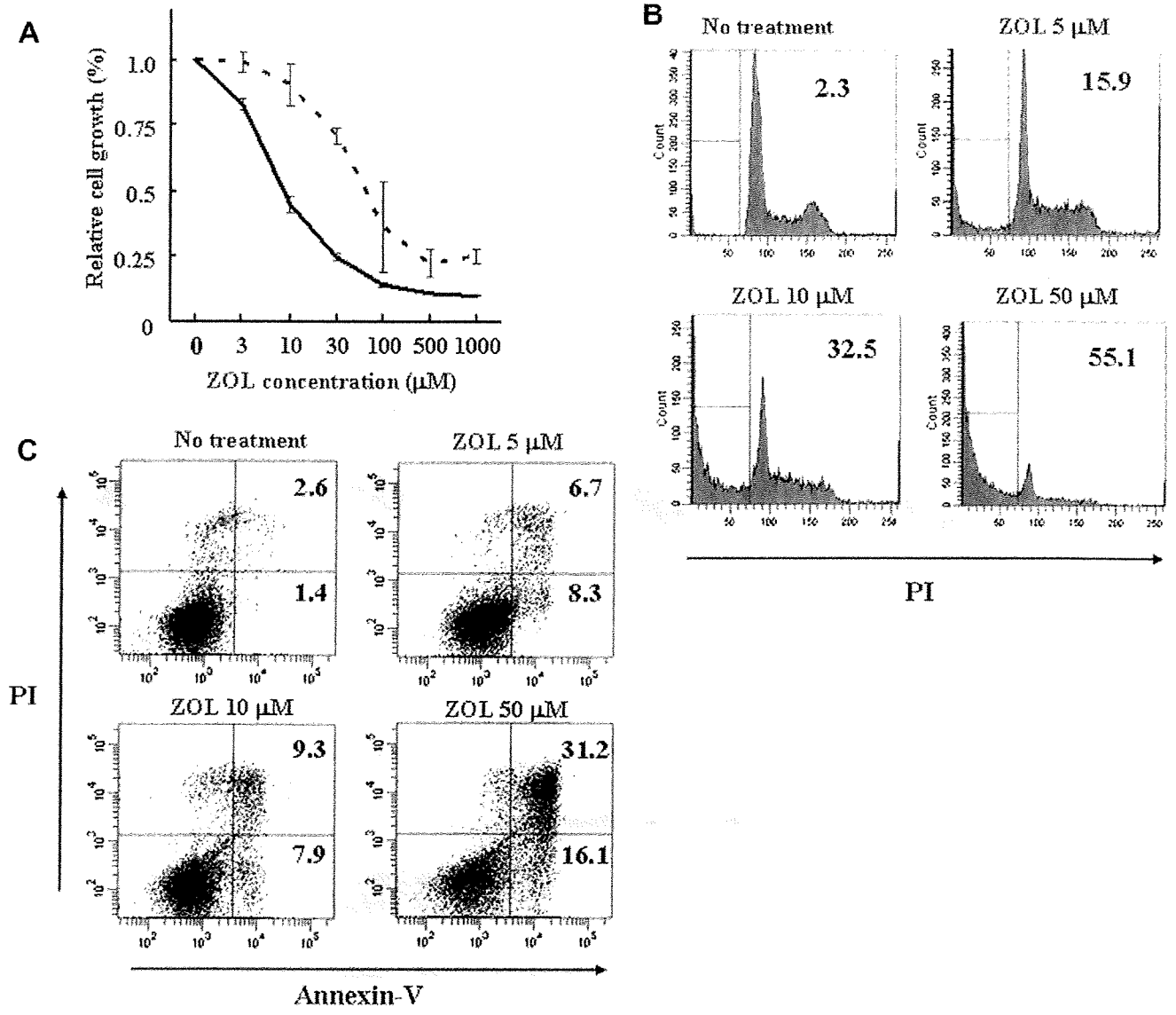

Fig. 4. ZOL treatment inhibits the proliferation of MM cells. (A) Cell proliferation was determined by the modified MTT assay as described in Section 2. ZOL treatment produced growth inhibitory effects in H2452 (solid line) and H28 (dotted line) MM cells in a dose-dependent manner. (B) Cell cycle analysis in H2452 MM cells using propidium iodide (PI) was performed after 72 h treatment with ZOL at the concentration indicated. Results are representative of three independent experiments. The numbers inside each histogram indicate the percentage of the subG1 fraction. (C) Determination of apoptosis induced by ZOL treatment at each concentration. Results are representative of three independent experiments. The numbers inside each quadrant indicate the percentage of the cell population with the quadrant characteristic.

IC_{50} which were obtained from the experiments above were used. We calculated the CIs and the Fa values at each dilution using the CalcuSyn soft as reported previously [33–36]. Dose-effect and CI–Fa plots illustrating the effects of PLK-1 siRNA and ZOL combinations are shown in Fig. 5C. As shown in the left panel of Fig. 5C, the treatment of PLK-1 siRNA combined with ZOL produced more growth inhibition than the treatments of each agent alone that are shown in Figs. 2B and 4A. The mathematically analyzed data of CI-Fa plots are shown in the right panel of Fig. 5C. In H2452 cells, the CI values at Fa 0.5, and 0.8 were 0.809 and 0.974, respectively; and in H28 cells, the CI values at Fa 0.5, and 0.8 were 0.082 and 0.836, respectively. These observations indicate that exposure to ZOL and the DNA-chimeric PLK-1 siRNA produced a synergistic effect on H2452 and H28 MM cell lines. We also investigated the alternation of the unprenylated RhoA expression in H2452 and H28 cells by the treatment of PLK-1 siRNA and ZOL. The combined treatment of concurrent PLK-1 siRNA and ZOL did not alter the unprenylated RhoA expression compared to the treatment of ZOL alone (Supplementary Fig. S1), suggesting that PLK-1 siRNA does not act on the prenylation of RhoA GTPase although PLK-1 siRNA diminishes PLK-1 expression.

4. Discussion

Synthetic siRNAs form complexes with liposomes, after which, the siRNA/liposome complex binds to the cell membrane and enters the cytoplasm via endocytosis. The complex then escapes from the endosome and releases its siRNA to the RNAi machinery [11,40]. Although single-stranded (ss) nucleic acids are rapidly degraded in serum or inside cells, ds nucleic acids are more stable than their

Please cite this article in press as: E. Kawata et al., A combination of a DNA-chimera siRNA against PLK-1 and zoledronic acid suppresses the growth of malignant mesothelioma cells *in vitro*, Cancer Lett. (2010), doi:10.1016/j.canlet.2010.02.008

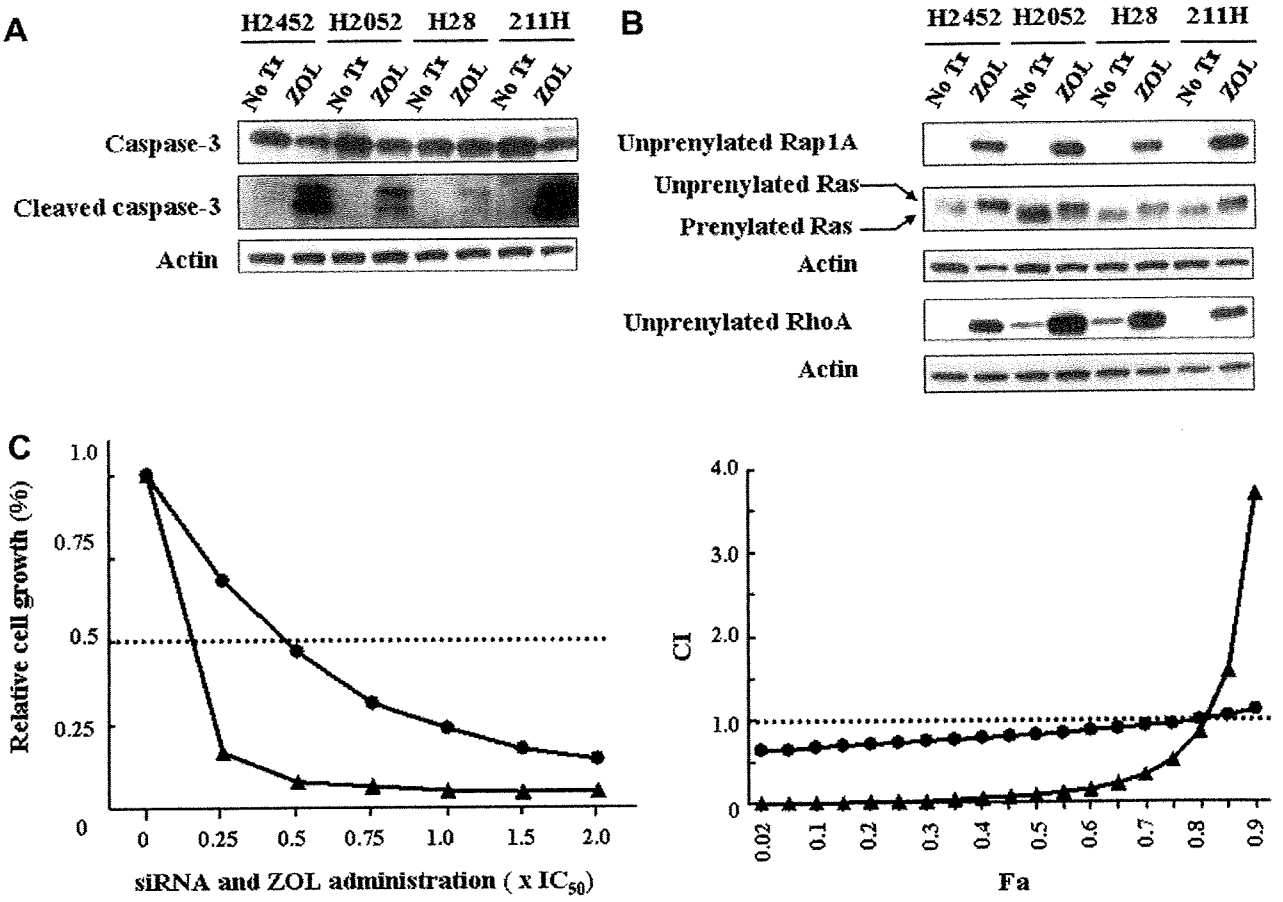

Fig. 5. Induction of apoptosis in MM cells by ZOL treatment (A and B) and combined effects of chimeric PLK-1 siRNA with ZOL. (A) Cleavage of caspase-3 by ZOL treatment. Four MM cell lines were incubated with ZOL at 50 μM for 72 h. Whole cell lysates were obtained and immunoblotting was performed as described in Section 2. (B) Evaluation of the inhibition of small GTPase protein prenylation by ZOL treatment (50 μM). Immunoblotting and immunoprecipitation were performed as described in Section 2. (C) Evaluation of the combined effects of DNA-chimeric PLK-1 siRNA and ZOL treatment on H2452 (filled circles) and H28 (filled triangles) mesothelioma cell lines. Cells were incubated for 72 h with six concentrations (0.25, 0.5, 0.75, 1.0, 1.5, or 2.0 times the IC_{50}) of each agent or both in combination using the constant ratio design followed by the modified MTT assay as described in Section 2. The IC_{50} values of PLK-1 siRNA for H2452 cells and H28 cells were 1.6 nM and 38.7 nM, respectively, and those of ZOL were 11.4 μM and 58.1 μM, respectively. Left panel: The killing curves of the concurrent administration of PLK-1 siRNA and ZOL. Right panel: Combination index (CI)-fraction affected (Fa) plots. Combination indexes were determined with the nonlinear regression program CalcuSyn.

ss counterparts; however, ds nucleic acids, including siRNAs, are still degraded and must be protected from endogenous nucleases in the bloodstream. Degradation can be avoided by the use of a suitable delivery system or by the nuclease-resistant chemical modification of the siRNA [10]. One approach involves the modification of the 2′-position of the ribose of the siRNA. Sugar modifications such as 2′-*O*-methylation, 2′-*O*-methoxyethylation, and 2′-fluoro-2′-deoxynucleoside modification can improve nuclease resistance [41,42]. Another approach involves the replacement of certain siRNA ribonucleotides with their deoxyribonucleotide counterparts.

We generated a DNA-chimeric siRNA, and substituted six basepairs from the 5′ end of the guide strand with their deoxyribonucleotide counterparts. This DNA-chimeric siRNA was more stable in human serum than the non-chimeric siRNA and showed resistance to endogenous nucleases. Moreover, the chimeric siRNA against PLK-1 decreased PLK-1 expression almost as effectively as the non-chimeric siRNA, and inhibited the proliferation of MM cells through the induction of apoptosis by cleaving caspase-3. These anti-neoplastic effects in the present study are consistent with our previous reports [19,20]. PLK-1 is overexpressed in MM cells compared to normal fibroblasts and, therefore, PLK-1 is a novel target that inhibits the proliferation of MM cells. Ui-Tei et al. [13] also demonstrated that DNA-chimeric siRNAs, in which the eight ribonucleotides from the 5′ end of the guide strand were substituted with deoxyribonucleotides, effectively induced gene-silencing without exerting the off-target effects. Our findings, taken together with the Ui-Tei's report, demonstrate that DNA-chimeric siRNAs result in safe and more effective gene-silencing and that the DNA-chimeric siRNA is much suitable for an *in vivo* administration. Further studies are warranted to evaluate the therapeutic potential of the DNA-chimeric siRNA *in vivo*.

ZOL, a third-generation BP, inhibits the activity of farnesyl diphosphate synthase in the mevalonate pathway, resulting in inhibition of the prenylation of small GTPases

Please cite this article in press as: E. Kawata et al., A combination of a DNA-chimera siRNA against PLK-1 and zoledronic acid suppresses the growth of malignant mesothelioma cells *in vitro*, Cancer Lett. (2010), doi:10.1016/j.canlet.2010.02.008

[24,25]. The prenylated small GTPases including Ras, Rap-1, and Rho proteins transduce signals downstream for cell functions such as cell proliferation, adhesion, and migration [43–45], while the inhibition of these small GTPase prenylation by BPs results in the suppression of cancer progression [26–30,46–48]. In the present study, we have revealed that ZOL also inhibits the proliferation of MM cells. Treatment of MM cells with ZOL inhibited the prenylation of Rap-1A, Ras, and RhoA proteins, and induced apoptosis by cleaving capsase-3. Other investigators have also reported that ZOL inhibits the proliferation of MM cells [49,50]. Interestingly, one report demonstrated that Ca^{2+} regulates the growth inhibitory effects of BPs on MM cells [49]. Calcification is a well-known feature in MM [51,52], and BPs accumulate rapidly in bone [24,25]. We have demonstrated previously that ZOL has anti-tumor effects against osteosarcoma [29,46]. These findings collectively suggest that malignancies with ossifying features, including MM and breast cancers [48], are suitable candidates for ZOL treatment.

PLK-1 regulates cell division at several points during the mitotic phase, and RhoA is also implicated in the regulation of cytokinesis. Prenylated Rho proteins are delivered to the plasma membrane and are concentrated at the cleavage furrow of the cell during the M phase of cell cycle [53,54]. PLK-1 regulates the local activation of RhoA to promote cytokinesis [38,39] and, therefore, we hypothesized that ZOL treatment would augment the cytotoxic efficacy of the PLK-1 siRNA in MM cells. The combined ZOL and PLK-1 siRNA treatment showed synergistic effects at both low (Fa 0.5) and high (Fa 0.8) concentrations.

In conclusion, a DNA-chimeric PLK-1 siRNA inhibited cellular proliferation and induced apoptosis in MM cells, and a combination of PLK-1 siRNA and ZOL treatment revealed synergistic inhibitory effects on MM cells. The observation reported in the present study indicates that PLK-1 is a novel target for the treatment of MM and that the DNA-chimeric siRNA against PLK-1 combined with ZOL treatment would be an attractive strategy in the fight against this aggressive disease.

Conflicts of interest

All authors declare that they have no conflicts of interest.

Acknowledgements

The authors thank Naoko Hashimoto for her excellent technical assistance. The authors also thank alphaGEN Co, Ltd (Tokyo, Japan) for designing DNA-chimeric siRNAs. The authors declare that they have no commercial affiliations. This work was partly supported by Research for Promoting Technological Seeds, Japan Science and Technology Agency, by a Grant-in-Aid for Scientific Research from the Ministry of Education, Culture, Sports, Science and Technology of Japan, and by the Kobayashi Institute for Innovative Cancer Chemotherapy.

Appendix A. Supplementary material

Supplementary data associated with this article can be found, in the online version, at doi:10.1016/j.canlet.2010.02.008.

References

[1] B.W. Robinson, R.A. Lake, Advances in malignant mesothelioma, New Engl. J. Med. 353 (2005) 1591–1603.
[2] J.C. Halstead, E. Lim, R.M. Venkateswaran, S.C. Charman, M. Goddard, A.J. Ritchie, Improved survival with VATS pleurectomy–decortication in advanced malignant mesothelioma, Eur. J. Surg. Oncol. 31 (2005) 314–320.
[3] D.A. Waller, Malignant mesothelioma – British surgical strategies, Lung Cancer 45 (Suppl 1) (2004) S81–S84.
[4] G. Carteni, C. Manegold, G.M. Garcia, S. Siena, C.C. Zielinski, D. Amadori, Y. Liu, J. Blatter, C. Visseren-Grul, R. Stahel, Malignant peritoneal mesothelioma – results from the international expanded access program using pemetrexed alone or in combination with a platinum agent, Lung Cancer 64 (2009) 211–218.
[5] P. Taylor, B. Castagneto, G. Dark, M. Marangolo, G.V. Scagliotti, R.J. van Klaveren, R. Labianca, M. Serke, W. Schuette, J.P. van Meerbeeck, D. Heigener, Y. Liu, S. Adachi, J. Blatter, J. von Pawel, Single-agent pemetrexed for chemonaive and pretreated patients with malignant pleural mesothelioma: results of an international expanded access program, J. Thorac. Oncol. 3 (2008) 764–771.
[6] P. Baas, A. Ardizzoni, F. Grossi, K. Nackaerts, G. Numico, E. Van Marck, M. van de Vijver, F. Monetti, M.J. Smid-Geirnaerdt, N. van Zandwijk, C. Debruyne, C. Legrand, G. Giaccone, The activity of raltitrexed (Tomudex) in malignant pleural mesothelioma: an EORTC phase II study (08992), Eur. J. Cancer 39 (2003) 353–357.
[7] J.P. van Meerbeeck, R. Gaafar, C. Manegold, R.J. Van Klaveren, E.A. Van Marck, M. Vincent, C. Legrand, A. Bottomley, C. Debruyne, G. Giaccone, Randomized phase III study of cisplatin with or without raltitrexed in patients with malignant pleural mesothelioma: an intergroup study of the European Organisation for Research and Treatment of Cancer Lung Cancer Group and the National Cancer Institute of Canada, J. Clin. Oncol. 23 (2005) 6881–6889.
[8] C.W. Lee, N. Murray, H. Anderson, S.C. Rao, W. Bishop, Outcomes with first-line platinum-based combination chemotherapy for malignant pleural mesothelioma: a review of practice in British Columbia, Lung Cancer 64 (2009) 308–313.
[9] Y. Aelony, Raltitrexed and pemetrexed studies in mesothelioma have not shown improved quality of life nor prolonged survival compared with effective pleurodesis with thoracoscopic talc poudrage, J. Clin. Oncol. 24 (2006) 4667 (author reply 4667–4668).
[10] D. Bumcrot, M. Manoharan, V. Koteliansky, D.W. Sah, RNAi therapeutics: a potential new class of pharmaceutical drugs, Nat. Chem. Biol. 2 (2006) 711–719.
[11] E. Ashihara, E. Kawata, T. Maekawa, Future prospect of RNA interference for cancer therapies, Curr. Drug Targets. in press.
[12] A. Boutla, C. Delidakis, I. Livadaras, M. Tsagris, M. Tabler, Short 5′-phosphorylated double-stranded RNAs induce RNA interference in Drosophila, Curr. Biol. 11 (2001) 1776–1780.
[13] K. Ui-Tei, Y. Naito, S. Zenno, K. Nishi, K. Yamato, F. Takahashi, A. Juni, K. Saigo, Functional dissection of siRNA sequence by systematic DNA substitution: modified siRNA with a DNA seed arm is a powerful tool for mammalian gene silencing with significantly reduced off-target effect, Nucleic Acids Res. 36 (2008) 2136–2151.
[14] S.M. Elbashir, J. Martinez, A. Patkaniowska, W. Lendeckel, T. Tuschl, Functional anatomy of siRNAs for mediating efficient RNAi in Drosophila melanogaster embryo lysate, Embo. J. 20 (2001) 6877–6888.
[15] F.A. Barr, H.H. Sillje, E.A. Nigg, Polo-like kinases and the orchestration of cell division, Nat. Rev. Mol. Cell Biol. 5 (2004) 429–440.
[16] B.C. van de Weerdt, R.H. Medema, Polo-like kinases: a team in control of the division, Cell Cycle 5 (2006) 853–864.
[17] K. Strebhardt, A. Ullrich, Targeting polo-like kinase 1 for cancer therapy, Nat. Rev. Cancer 6 (2006) 321–330.
[18] N. Takai, R. Hamanaka, J. Yoshimatsu, I. Miyakawa, Polo-like kinases (Plks) and cancer, Oncogene 24 (2005) 287–291.
[19] M. Nogawa, T. Yuasa, S. Kimura, M. Tanaka, J. Kuroda, K. Sato, A. Yokota, H. Segawa, Y. Toda, S. Kageyama, T. Yoshiki, Y. Okada, T. Maekawa, Intravesical administration of small interfering RNA

Please cite this article in press as: E. Kawata et al., A combination of a DNA-chimera siRNA against PLK-1 and zoledronic acid suppresses the growth of malignant mesothelioma cells *in vitro*, Cancer Lett. (2010), doi:10.1016/j.canlet.2010.02.008

targeting PLK-1 successfully prevents the growth of bladder cancer, J. Clin. Invest. 115 (2005) 978–985.
[20] E. Kawata, E. Ashihara, S. Kimura, K. Takenaka, K. Sato, R. Tanaka, A. Yokota, Y. Kamitsuji, M. Takeuchi, J. Kuroda, F. Tanaka, T. Yoshikawa, T. Maekawa, Administration of PLK-1 small interfering RNA with atelocollagen prevents the growth of liver metastases of lung cancer, Mol. Cancer Ther. 7 (2008) 2904–2912.
[21] P. Schoffski, Polo-like kinase (PLK) inhibitors in preclinical and early clinical development in oncology, Oncologist 14 (2009) 559–570.
[22] K. Mross, A. Frost, S. Steinbild, S. Hedbom, J. Rentschler, R. Kaiser, N. Rouyrre, D. Trommeshauser, C.E. Hoesl, G. Munzert, Phase I dose escalation and pharmacokinetic study of BI 2536, a novel polo-like kinase 1 inhibitor, in patients with advanced solid tumors, J. Clin. Oncol. 26 (2008) 5511–5517.
[23] B. Spankuch-Schmitt, J. Bereiter-Hahn, M. Kaufmann, K. Strebhardt, Effect of RNA silencing of polo-like kinase-1 (PLK1) on apoptosis and spindle formation in human cancer cells, J. Natl. Cancer Inst. 94 (2002) 1863–1877.
[24] T. Yuasa, S. Kimura, E. Ashihara, T. Habuchi, T. Maekawa, Zoledronic acid – a multiplicity of anti-cancer action, Curr. Med. Chem. 14 (2007) 2126–2135.
[25] J.R. Green, Bisphosphonates: preclinical review, Oncologist 9 (Suppl 4) (2004) 3–13.
[26] J. Kuroda, S. Kimura, H. Segawa, Y. Kobayashi, T. Yoshikawa, Y. Urasaki, T. Ueda, F. Enjo, H. Tokuda, O.G. Ottmann, T. Maekawa, The third-generation bisphosphonate zoledronate synergistically augments the anti-Ph+ leukemia activity of imatinib mesylate, Blood 102 (2003) 2229–2235.
[27] S. Matsumoto, S. Kimura, H. Segawa, J. Kuroda, T. Yuasa, K. Sato, M. Nogawa, F. Tanaka, T. Maekawa, H. Wada, Efficacy of the third-generation bisphosphonate, zoledronic acid alone and combined with anti-cancer agents against small cell lung cancer cell lines, Lung Cancer 47 (2005) 31–39.
[28] T. Yuasa, M. Nogawa, S. Kimura, A. Yokota, K. Sato, H. Segawa, J. Kuroda, T. Maekawa, A third-generation bisphosphonate, minodronic acid (YM529), augments the interferon alpha/beta-mediated inhibition of renal cell cancer cell growth both in vitro and in vivo, Clin. Cancer Res. 11 (2005) 853–859.
[29] N. Horie, H. Murata, Y. Nishigaki, T. Matsui, H. Segawa, M. Nogawa, T. Yuasa, S. Kimura, T. Maekawa, S. Fushiki, T. Kubo, The third-generation bisphosphonates inhibit proliferation of murine osteosarcoma cells with induction of apoptosis, Cancer Lett. 238 (2006) 111–118.
[30] K. Sato, T. Yuasa, M. Nogawa, S. Kimura, H. Segawa, A. Yokota, T. Maekawa, A third-generation bisphosphonate, minodronic acid (YM529), successfully prevented the growth of bladder cancer in vitro and in vivo, Brit. J. Cancer 95 (2006) 1354–1361.
[31] T.C. Chou, Drug combination studies and their synergy quantification using the Chou-Talalay method, Cancer Res. 70 (2010) 440–446.
[32] T.C. Chou, Theoretical basis, experimental design, and computerized simulation of synergism and antagonism in drug combination studies, Pharmacol. Rev. 58 (2006) 621–681.
[33] S. Kimura, J. Kuroda, H. Segawa, K. Sato, M. Nogawa, T. Yuasa, O.G. Ottmann, T. Maekawa, Antiproliferative efficacy of the third-generation bisphosphonate, zoledronic acid, combined with other anticancer drugs in leukemic cell lines, Int. J. Hematol. 79 (2004) 37–43.
[34] O.H. Temmink, E.K. Hoebe, K. van der Born, S.P. Ackland, M. Fukushima, G.J. Peters, Mechanism of trifluorothymidine potentiation of oxaliplatin-induced cytotoxicity to colorectal cancer cells, Brit. J. Cancer 96 (2007) 231–240.
[35] N. Keshelava, E. Davicioni, Z. Wan, L. Ji, R. Sposto, T.J. Triche, C.P. Reynolds, Histone deacetylase 1 gene expression and sensitization of multidrug-resistant neuroblastoma cell lines to cytotoxic agents by depsipeptide, J. Natl. Cancer Inst. 99 (2007) 1107–1119.
[36] S. Sei, J.K. Mussio, Q.E. Yang, K. Nagashima, R.E. Parchment, M.C. Coffey, R.H. Shoemaker, J.E. Tomaszewski, Synergistic antitumor activity of oncolytic reovirus and chemotherapeutic agents in non-small cell lung cancer cells, Mol. Cancer 8 (2009) 47.
[37] A.A. Reszka, J. Halasy-Nagy, G.A. Rodan, Nitrogen-bisphosphonates block retinoblastoma phosphorylation and cell growth by inhibiting the cholesterol biosynthetic pathway in a keratinocyte model for esophageal irritation, Mol. Pharmacol. 59 (2001) 193–202.
[38] B.N. Dai, Y. Yang, Z. Chau, M. Jhanwar-Uniyal, Polo-like kinase 1 regulates RhoA during cytokinesis exit in human cells, Cell Proliferat. 40 (2007) 550–557.
[39] M.E. Burkard, C.L. Randall, S. Larochelle, C. Zhang, K.M. Shokat, R.P. Fisher, P.V. Jallepalli, Chemical genetics reveals the requirement for polo-like kinase 1 activity in positioning RhoA and triggering cytokinesis in human cells, Proc. Natl. Acad. Sci. USA 104 (2007) 4383–4388.
[40] O. Zelphati, F.C. Szoka Jr., Mechanism of oligonucleotide release from cationic liposomes, Proc. Natl. Acad. Sci. USA 93 (1996) 11493–11498.
[41] S. Choung, Y.J. Kim, S. Kim, H.O. Park, Y.C. Choi, Chemical modification of siRNAs to improve serum stability without loss of efficacy, Biochem. Biophys. Res. Commun. 342 (2006) 919–927.
[42] M.A. Behlke, Chemical modification of siRNAs for in vivo use, Oligonucleotides 18 (2008) 305–319.
[43] W.J. Chia, B.L. Tang, Emerging roles for Rab family GTPases in human cancer, Biochim. Biophys. Acta 1795 (2009) 110–116.
[44] M. Hattori, N. Minato, Rap1 GTPase: functions, regulation, and malignancy, J. Biochem. 134 (2003) 479–484.
[45] N. Fehrenbacher, D. Bar-Sagi, M. Philips, Ras/MAPK signaling from endomembranes, Mol. Oncol. 3 (2009) 297–307.
[46] K. Koto, N. Horie, S. Kimura, H. Murata, T. Sakabe, T. Matsui, M. Watanabe, S. Adachi, T. Maekawa, S. Fushiki, T. Kubo, Clinically relevant dose of zoledronic acid inhibits spontaneous lung metastasis in a murine osteosarcoma model, Cancer Lett. 274 (2009) 271–278.
[47] S. Yano, H. Zhang, M. Hanibuchi, T. Miki, H. Goto, H. Uehara, S. Sone, Combined therapy with a new bisphosphonate, minodronate (YM529), and chemotherapy for multiple organ metastases of small cell lung cancer cells in severe combined immunodeficient mice, Clin. Cancer Res. 9 (2003) 5380–5385.
[48] T. Hiraga, P.J. Williams, A. Ueda, D. Tamura, T. Yoneda, Zoledronic acid inhibits visceral metastases in the 4T1/luc mouse breast cancer model, Clin. Cancer Res. 10 (2004) 4559–4567.
[49] M.A. Merrell, S. Wakchoure, J.M. Ilvesaro, K. Zinn, B. Gehrs, P.P. Lehenkari, K.W. Harris, K.S. Selander, Differential effects of Ca(2+) on bisphosphonate-induced growth inhibition in breast cancer and mesothelioma cells, Eur. J. Pharmacol. 559 (2007) 21–31.
[50] S. Wakchoure, M.A. Merrell, W. Aldrich, T. Millender-Swain, K.W. Harris, P. Triozzi, K.S. Selander, Bisphosphonates inhibit the growth of mesothelioma cells in vitro and in vivo, Clin. Cancer Res. 12 (2006) 2862–2868.
[51] A. Raizon, A. Schwartz, W. Hix, S.D. Rockoff, Calcification as a sign of sarcomatous degeneration of malignant pleural mesotheliomas: a new CT finding, J. Comput. Assist. Tomogr. 20 (1996) 42–44.
[52] F. Liu, P. Misra, E.P. Lunsford, J.T. Vannah, Y. Liu, R.E. Lenkinski, J.V. Frangioni, A dose- and time-controllable syngeneic animal model of breast cancer microcalcification, Breast Cancer Res. Treat. (2009).
[53] F.A. Barr, U. Gruneberg, Cytokinesis: placing and making the final cut, Cell 131 (2007) 847–860.
[54] S. Yoshida, S. Bartolini, D. Pellman, Mechanisms for concentrating Rho1 during cytokinesis, Genes Dev. 23 (2009) 810–823.

Please cite this article in press as: E. Kawata et al., A combination of a DNA-chimera siRNA against PLK-1 and zoledronic acid suppresses the growth of malignant mesothelioma cells *in vitro*, Cancer Lett. (2010), doi:10.1016/j.canlet.2010.02.008

Biochemical and Biophysical Research Communications 393 (2010) 498–503

Contents lists available at ScienceDirect

Biochemical and Biophysical Research Communications

journal homepage: www.elsevier.com/locate/ybbrc

Use of bicistronic vectors in combination with flow cytometry to screen for effective small interfering RNA target sequences

Naoka Kamio [a,b,1], Hideyo Hirai [a,b,*,1], Eishi Ashihara [a], Daniel G. Tenen [c,d], Taira Maekawa [a], Jiro Imanishi [b]

[a] Department of Transfusion Medicine and Cell Therapy, Kyoto University Hospital, 54 Kawahara-cho, Shogoin, Sakyo-ku, Kyoto 606-8507, Japan
[b] Department of Microbiology and Immunology, Kyoto Prefectural University of Medicine, 465 Kajii-cho, Kamigyo-ku, Kyoto 606-8566, Japan
[c] Harvard Stem Cell Institute, Harvard Medical School, Boston, MA 02115, USA
[d] Cancer Science Institute, National University of Singapore, Singapore 117456, Singapore

ARTICLE INFO

Article history:
Received 1 February 2010
Available online 10 February 2010

Keywords:
Bicistronic vector
Flow cytometry
siRNA
Green fluorescent protein

ABSTRACT

The efficacy and specificity of small interfering RNAs (siRNAs) are largely dependent on the siRNA sequence. Since only empirical strategies are currently available for predicting these parameters, simple and accurate methods for evaluating siRNAs are needed. To simplify such experiments, target genes are often tagged with reporters for easier readout. Here, we used a bicistronic vector expressing a target gene and green fluorescent protein (GFP) to create a system in which the effect of an siRNA sequence was reflected in the GFP expression level. Cells were transduced with the bicistronic vector, expression vectors for siRNA and red fluorescent protein (RFP). Flow cytometric analysis of the transduced cells revealed that siRNAs for the target gene silenced GFP from the bicistronic vector, but did not silence GFP transcribed without the target gene sequence. In addition, the mean fluorescence intensities of GFP on RFP-expressing cells correlated well with the target gene mRNA and protein levels. These results suggest that this flow cytometry-based method enables us to quantitatively evaluate the efficacy and specificity of siRNAs. Because of its simplicity and effectiveness, this method will facilitate the screening of effective siRNA target sequences, even in high-throughput applications.

Introduction

RNA interference is a sequence-specific posttranscriptional gene-silencing process induced by short double-stranded RNA [1,2]. This evolutionally conserved phenomenon is widely applied to the functional analysis of genes and to therapeutic trials [3–7]. The specificity and efficacy of gene silencing with short interfering RNAs (siRNA) are largely dependent on the siRNA sequence. Accumulating evidence suggests that only a limited number of siRNAs are capable of inducing highly effective target gene silencing in a sequence-specific manner [8–11]. Many algorithms and guidelines have been developed for the design of effective siRNA sequences [12–16]. However, predicting siRNA efficacy and specificity remains empirical and requires experimental verification. Therefore, simple and accurate methods for evaluating siRNAs are required.

To directly measure the protein or mRNA levels of a target gene, gene-specific reagents, such as primers or antibodies, and precisely optimized experimental conditions for each target gene are necessary. To avoid such complicating steps, target genes can instead be tagged with various reporter genes for easier readout. When a target gene sequence is followed by the combined sequences of an internal ribosome entry site (IRES) and green fluorescence protein (GFP) in an expression vector, then the target gene and GFP are transcribed as a single mRNA and are translated independently in the cell [17,18]. Once an siRNA against the target gene is transduced together with the bicistronic expression vector, the siRNA will essentially destroy the entire mRNA, including the target gene and GFP. The GFP expression level is then expected to reflect the efficacy of the siRNA (Fig. 1).

Here, we utilized a GFP-expressing bicistronic vector to report the effect of an siRNA, and investigated whether the siRNA efficiency and specificity could be quantitatively monitored by flow cytometry.

Materials and methods

Cell culture. HEK293 cells were grown in Dulbecco's minimum essential medium supplemented with 10% fetal calf serum (FCS) at 37 °C in 100% humidified air.

siRNA design. siRNA sequences against the mouse cyclic AMP-responsive element modulator (CREM) gene were designed using the online siRNA design software programs siRNA Target Finder

* Corresponding author. Address: Department of Transfusion Medicine and Cell Therapy, Kyoto University Hospital, 54 Kawahara-cho, Shogoin, Sakyo-ku, Kyoto 606-8507, Japan. Fax: +81 75 751 4283.
E-mail address: hhirai@kuhp.kyoto-u.ac.jp (H. Hirai).

[1] These authors contributed equally to this work.

0006-291X/$ - see front matter © 2010 Elsevier Inc. All rights reserved.
doi:10.1016/j.bbrc.2010.02.033

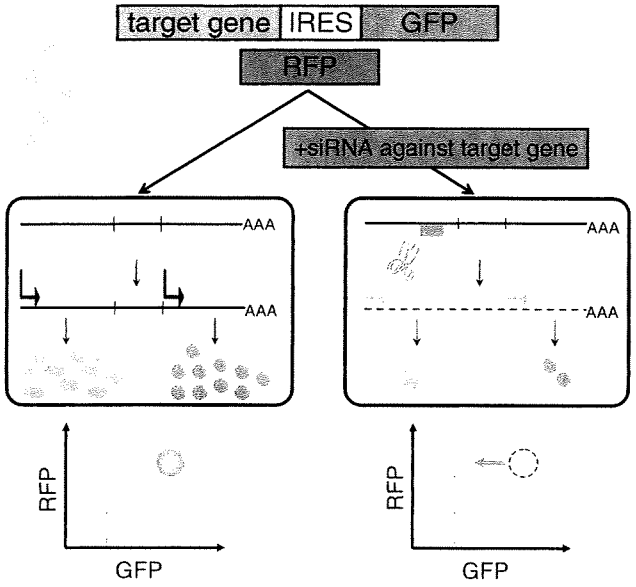

Fig. 1. Strategy and experimental design. The target gene and GFP are transcribed as a single mRNA from a bicistronic vector and translated independently (left panel). An siRNA against the target gene destroys the entire mRNA, including the target gene and GFP expressed from the bicistronic vector. The GFP expression level should reflect the effects of the siRNA (right panel). RFP is expressed from an independent vector.

(Ambion; http://www.ambion.com/jp/techlib/misc/siRNA_finder.html) and siDESIGN Center (Thermo Scientific; http://www.dharmacon.com/DesignCenter/DesignCenterPage.aspx). We chose three different 19-bp sequences that follow AA and contain GC sequences at less than a 50% frequency. The sequences were as follows: CREM#1, ggcaaatgaccatggaaa; CREM#2, gtaattgattcgcataaac; and CREM#3, gaagcaactcgcaagcggg. The siRNA sequences against firefly luciferase (GL3) and GFP were cttacgctgagtacttcga and caagctgaccctgaagttc, respectively.

Vector construction. Total RNA was extracted from a C57BL/6 mouse testis and reverse transcribed using the ReverTraAce kit (TOYOBO, Japan). The mouse CREM gene was amplified by PCR from the cDNA using the following primers: sense, gcgaattcatgagcaaatgtggcaggaaaaagtatatgagg; and anti-sense, ggctcggttactctgctttatggcaataa. The PCR product was digested with EcoRI and XhoI and cloned into the EcoRI–XhoI site of the retrovirus vector MSCV-IRES-GFP (pMIG). For red fluorescence protein (RFP) expression, pDsRed-Monomer-Hyg-N1 (pRFP, Clontech, CA) was used. The SiVM2 vector, in which a short hairpin RNA is driven by a human H1 promoter, was used for siRNA expression [19].

We used the following oligonucleotides encoding mouse CREM-specific siRNAs: (CREM#1), 5′-TCC CGG CAA ATG ACC ATG GAA ACT TCA AGA GAG TTT CCA TGG TCA TTT CCC T-3′ and 5′-GGC AAA TGA CTG GAA ACT CTC TTG AAG TTT CCA TGG TCA TTT GCC-3′; (CREM#2), 5′-TCC CGT AAT TGA TTC GCA TAA ACT TCA AGA GAG TTT ATG CGA ATC AAT TAC T-3′ and 5′-GTA ATT GAT TCG CAT AAA CTC TCT TGA AGT TTA TGC GAA TCA ATT AC-3′; and (CREM#3), 5′-TCC CGA AGC AAC TCG CAA GCG GGT TCA AGA GAC CCG CTT GCG AGT TGC TTC T-3′ and 5′-GAA GCA ACT CGC AAG CGG GTC TCT TGA ACC CGC TGC GAT TGC TTC-3′. These oligonucleotides were annealed and subcloned downstream of the H1 promoter using BbsI and XcmI in the SiVM2 vector [19].

Transfection. HEK293 cells were transduced with various combinations of plasmid vectors using the Lipofectamine LTX and Plus reagents (Invitrogen, CA) according to the manufacturer's protocol. Briefly, cells were seeded 24-h prior to transfection into a 6-well plate at a density of 1×10^5/well. One microgram of DNA was mixed with 2.5 μl of Lipofectamine LTX and 1 μl of Plus reagent in 200 μl of OPTI-MEM medium, incubated at room temperature for 30 min, and then added to each well of the 6-well plate. The fluorescence of GFP and RFP were monitored using an Olympus IX71 microscope, and data were captured with DP controller/Manager software (Olympus, Japan).

Flow cytometry. Twenty-four hours after transfection, the cells were washed with phosphate buffered saline (PBS), treated with 0.05% trypsin/EDTA, and resuspended in PBS supplemented with 2% FCS. Flow cytometric analysis was carried out using FACSCalibur (BD). To calibrate our flow cytometry results, mock-transfected cells and cells transduced with either pMIG or pRFP alone were included with every experiment. Data were analyzed using FlowJo software (Tree Star, Inc.).

Real-time PCR. RNA was extracted from cells using the RNeasy Micro kit (Qiagen) according to the manufacturer's protocol, and was reverse transcribed using a random hexamer primer. Quantitative PCR was performed using the Light Cycler Taqman Master kit (Roche). The CREM expression was normalized to GAPDH expression. The primers and probes used were as follows: (mouse CREM) left, gctgaggctgatgaaaaaca, right, gccacacgattttcaagaca, universal probe library (UPL) #4; (GAPDH) left, tgtccgtcgtggatctac, right, cctgcttcaccaccttcttg, UPL #80.

Western blotting. We used anti-CREM (sc-440 X, Santa Cruz), anti-actin (sc7210, Santa Cruz), and HRP-conjugated anti-rabbit (sc-2317, Santa Cruz) antibodies for Western blotting. Band intensities were quantified using Image J software (http://rsb.info.nih.gov/ij/).

Results

To verify that the GFP expression level could be evaluated by flow cytometry, we first examined siRNA directly targeted to GFP. An MSCV-based vector (MSCV-IRES-GFP: pMIG) was utilized as our GFP expression vector. An siRNA sequence against GFP was cloned into the siVM2 expression vector, in which siRNA was driven by a human H1 promoter (siVM2GFP) [19]. A red RFP monomer expression vector (pDsRed-Momoner-Hyg-N1: pRFP) was used to normalize the transduction efficiency.

HEK293 cells were transduced with pRFP and pMIG with or without siVM2GFP, and the GFP and RFP expression levels were evaluated by fluorescent microscopy and flow cytometry 24 h after transfection (Fig. 2A and B, respectively). When the RFP expression vector was co-transduced with GFP, most RFP-positive cells expressed GFP, as expected (middle panels in Fig. 2A and B). The GFP expression was highly suppressed when siVM2GFP was co-transduced (bottom panels in Fig. 2A and B). In contrast, the RFP expression level was not affected by addition of the GFP-targeted siRNA expression vector, suggesting that the use of RFP is appropriate for correcting the transduction efficiency.

Fig. 2C displays the mean fluorescent intensities (MFIs) for GFP within RFP-positive cells. The solid and dotted lines represent GFP expression with or without the GFP expression vector, respectively, while the shaded line represents GFP expression in RFP-positive cells transduced with the siRNA expression vector. The MFIs for each condition were: 5.06 for pRFP only, 226 for pMIG + pRFP, and 37.5 for siVM2GFP + pMIG + pRFP. The siRNA efficiency was calculated as 85.3%, according to the following equation: siRNA efficiency = (MFIpMIG + pRFP − MFIpMIG + pRFP + siVM2)/(MFIpMIG + pRFP − MFIpRFPonly). These results suggest that the GFP expression level within RFP-positive cells could be examined at the single cell level by flow cytometry.

Using this system, we assessed three different siRNA sequences targeting the mouse CREM protein. CREM is a member of the cyclic

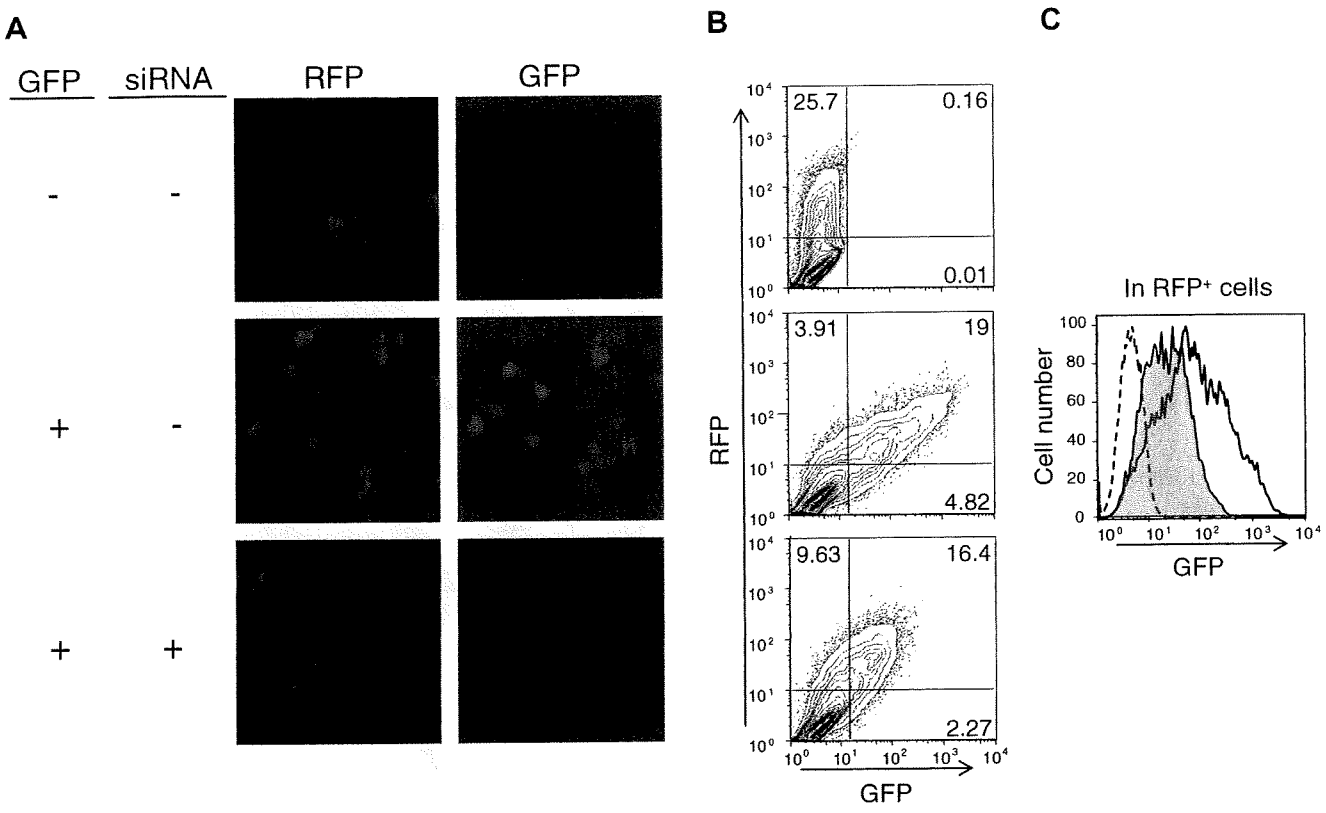

Fig. 2. Flow cytometry-based quantification of GFP expression using GFP-targeted siRNA. HEK293 cells were transduced with an RFP expression vector, co-transduced with or without a GFP and/or an siRNA expression vector, as indicated. Fluorescence was monitored 24 h after transduction by fluorescent microscopy (A) or flow cytometry (B and C). The mean fluorescent intensities (MFI) of GFP in the RFP-positive cells were plotted in (C). The solid and dotted lines represent GFP expression within RFP-positive cells with or without the GFP expression vector, respectively. The GFP expression levels with the siRNA expression vectors are represented by the shaded lines. Results are representative of three independent experiments.

AMP responsive element binding (CREB) protein family of transcription factors. The siRNAs were designed to target the mouse CREM (NM_013498) coding sequence at 308-, 469-, and 817-bp. As a non-specific siRNA control, we used siRNA targeted to firefly luciferase (GL3, Promega). Fig. 3A shows the GFP and RFP expression levels in cells transduced with a GFP expression vector without mouse CREM sequences (pMIG). None of the siRNAs affected the GFP or RFP expression levels (Fig. 3A, left panel). The solid and dotted lines in Fig. 3A (right panels) represent the GFP expression in RFP-positive cells with or without pMIG, respectively. The shaded lines represent the GFP expression levels with transduction of the siRNA expression vectors. The GFP expression within RFP-positive cells was not repressed by any siRNA vector.

Next, HEK293 cells were transduced with pRFP and a bicistronic CREM expression vector (pMIG-mCREM), with or without an siRNA expression vector. CREM-targeted, but not luciferase-targeted, siRNAs specifically repressed GFP expression (Fig. 3B, left panels). The GFP expression levels of RFP-positive cells are plotted in the right panels of Fig. 3B. The solid and dotted lines represent GFP expression within RFP-positive cells transduced with or without pMIG-mCREM, respectively. The shaded lines represent GFP expression with transduction of the siRNA expression vectors. The MFIs for each condition were as follows: 6.19 for pRFP only, 59 for pMIG-mCREM + pRFP, 46.4 for pMIG-mCREM + pRFP + siVM2GL3, 9.59 for pMIG-mCREM + pRFP + siVM2CREM#1, 8.88 for pMIG-mCREM + pRFP + siVM2CREM#2, and 14.8 for pMIG-mCREM + pRFP + siVM2CREM#3 (Fig. 3B, right panels). All three siRNA sequences targeting mouse CREM (CREM#1, #2, and #3) effectively suppressed GFP expression in RFP-positive cells compared to the control (no siRNA expression vector), with efficiencies of 93.5%, 94.9%, and 83.6%, respectively. The siRNA for firefly luciferase did not affect GFP expression. These results suggest that the effects of the siRNA vectors on the GFP expression level were specific to the CREM sequence located in front of the IRES sequence, and not to the GFP sequence.

To verify our screening method, we measured the mRNA and protein expression levels using real-time PCR and Western blotting, respectively (Fig. 4B–D). The total RNAs and proteins for the measurement were extracted from the same samples as used in the flow cytometric analysis. Both the mRNA and protein expression levels of CREM correlated very well with the relative MFI for GFP in RFP-positive cells (Fig. 4E and F, $R^2 = 0.9537$ and 0.9171, respectively). We also verified the feasibility of the system by applying it to four other genes (data not shown).

Discussion

In this study, we successfully evaluated the efficacy and specificity of siRNAs by monitoring the fluorescent proteins expressed from bicistronic vectors by flow cytometry.

Various reporter genes have been utilized for siRNA screening [20–24]. The advantages of using targeted reporter genes over direct measurements are many. For instance, the siRNA efficiency can be evaluated even when target gene-specific reagents such as antibodies are not available. Furthermore, when a target gene is expressed at very low levels by the cells, the effect of an siRNA can be difficult to evaluate by direct measurement of the RNA or proteins. Enhancement of target gene expression by vectors en-

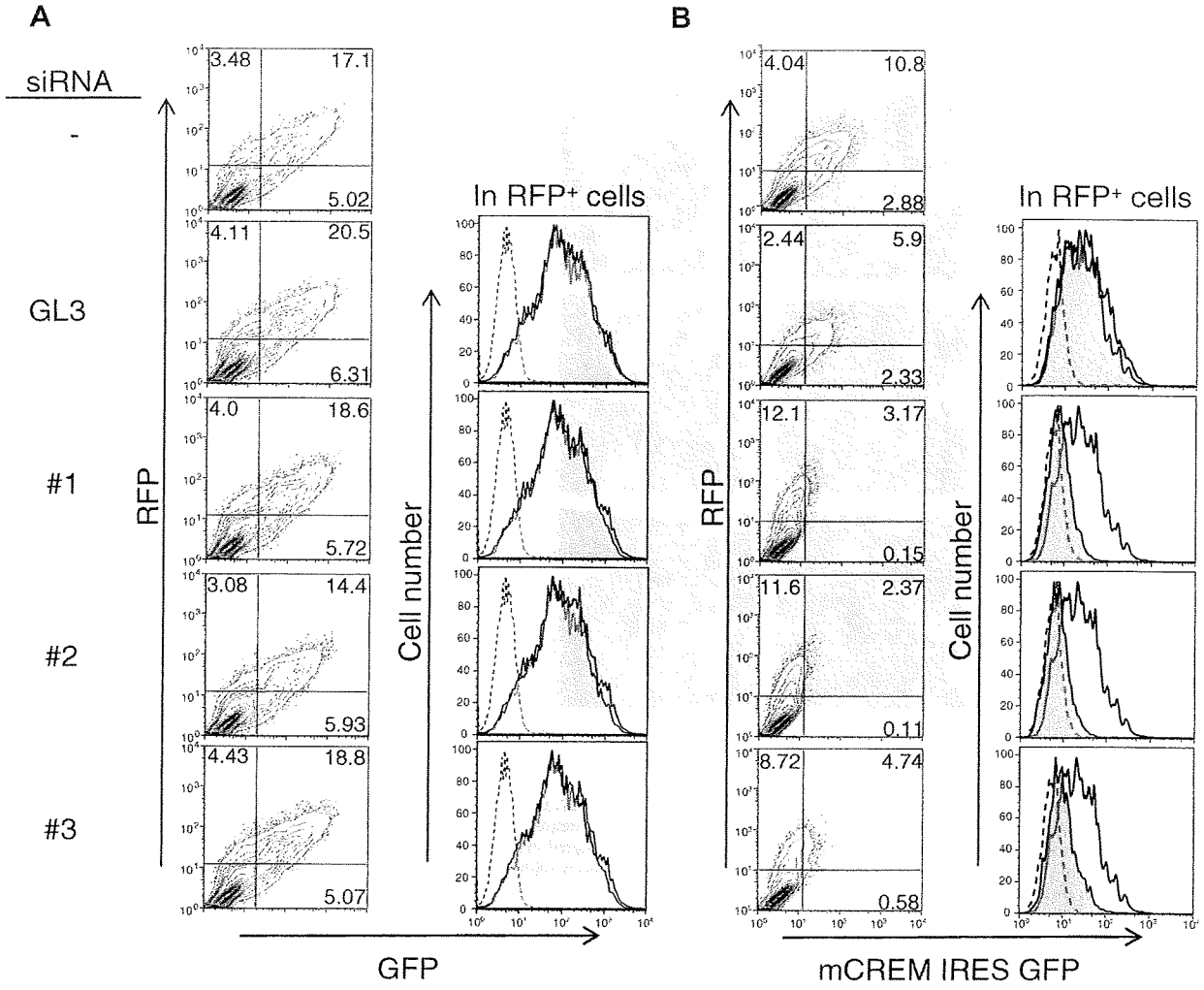

Fig. 3. Flow cytometry-based method for screening for an effective siRNA against the mouse CREM gene. (A) HEK293 cells were transduced with an RFP vector and a GFP expression vector with or without one of the siRNA expression vectors (firefly luciferase [GL3], CREM#1, CREM#2, or CREM#3). Flow cytometry data analyzed 24 h after transduction are shown in the left panels. The RFP-positive cells (left panels) were analyzed for GFP expression (right panels). The solid and dotted lines represent GFP expression within RFP-positive cells with or without pMIG, respectively. (B) HEK293 cells were transduced with the pRFP vector and a bicistronic CREM expression vector (CREM + GFP) with or without one of the siRNA expression vectors (firefly luciferase [GL3], CREM#1, CREM#2, or CREM#3). Results are representative of three independent experiments.

ables us to avoid such problems. Low transduction efficiencies also complicate the evaluation of the effects of an siRNA. Direct measurements typically assess the gene expression level in a cell mass, and not on an individual cell basis. By using flow cytometry, fluorescent proteins of multiple wavelengths can be monitored simultaneously after the simple manipulation of cells [24]. The intensities of the multiple fluorescences from a single cell can be quantitatively monitored and recorded. In this study, fluorescence intensities representing the efficacy of siRNAs (GFP) and the transduction (RFP) were monitored simultaneously from a single cell by flow cytometry, resulting in single cell-based quantification. By monitoring the GFP level of RFP-positive cells, problems arising from low transduction efficiencies could be avoided. Flow cytometric analyses were performed 24 h after transfection, and did not require RNA or protein extractions, which are time- and labor-consuming processes. Cells were simply treated with trypsin and EDTA and then directly analyzed. Each process step was very simple and was performed within a fairly short time. These features of the experimental process are suitable for high-throughput assay.

We utilized bicistronic expression vectors to indicate target gene expression rather than target-fused fluorescent reporter genes. Bicistronic vectors are already widely used in many fields, and cloning is easier to perform than the fusion process. The stability of GFP expressed from a bicistronic vector is theoretically constant irrespective of the target genes. Optimization of the time course of the experiment is unnecessary because of the consistency of protein stability. In addition, GFP repression by an siRNA against a target gene is mediated at the mRNA level and not after translation, since the target gene and GFP are transcribed as a single mRNA and are translated in different ways (cap-dependent and -independent translation, respectively) [25,26]. Therefore, RNA interference-dependent gene silencing can be more precisely monitored than is possible using the fusion system.

In summary, we have devised a novel flow cytometry-based method to evaluate the effects of siRNAs. Cell samples for flow cytometry are prepared by transducing siRNA and a bicistronic vector, which expresses GFP and the target gene, together with an RFP expression vector. The simplicity of this flow cytometry-

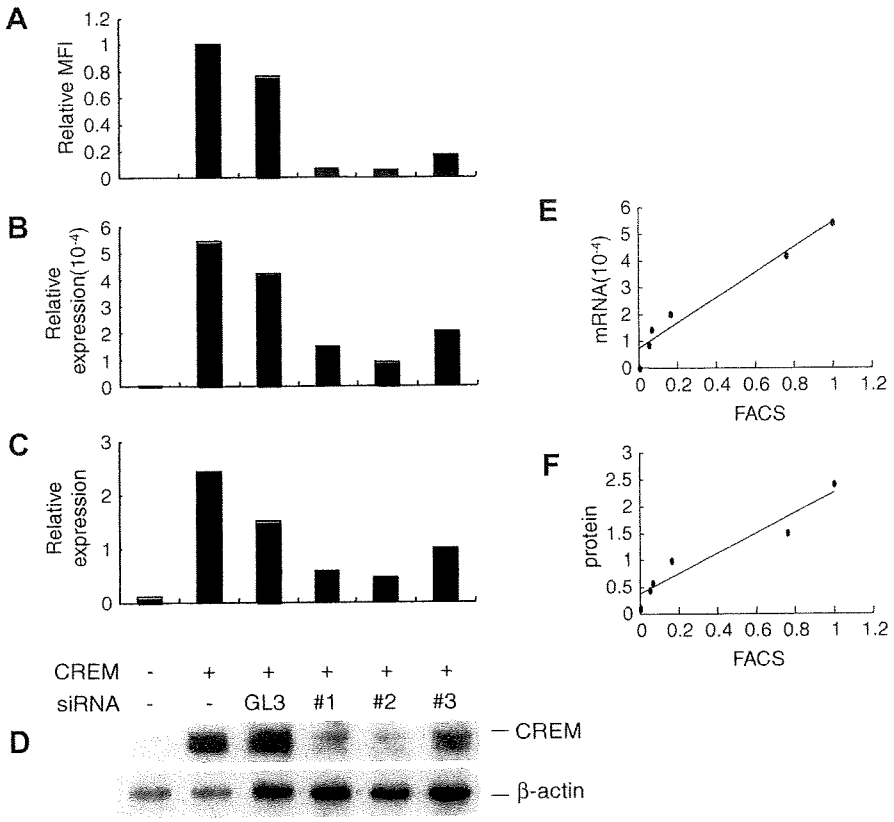

Fig. 4. Verification of the flow cytometry-based method by conventional methods. HEK293 cells were transduced with an RFP vector and a bicistronic CREM expression vector (CREM + GFP), with or without one of the siRNA expression vectors (firefly luciferase [GL3], CREM#1, CREM#2, or CREM#3). (A) Flow cytometric analysis 24 h after transduction. Mean fluorescent intensities of GFP in RFP-positive cells. (B) Relative expression level of mRNA for the mouse CREM gene, normalized to GAPDH. (C and D) Western blotting results. The band densities in (D) were quantified using Image J software (C). (E and F) The MFI was correlated with the mRNA (R^2 = 0.9537) (E) or protein expression (R^2 = 0.9171) (F). Results are representative of three independent experiments.

based method will facilitate the screening of effective siRNA sequences.

Acknowledgments

We thank Drs. S. Mizuno and K. Akashi for generously providing us with siVM2 vector. This work was supported by the Mitsubishi Foundation to H.H.; and Kakenhi [Grant Nos. 21591246 to H.H. and 21590443 to J.I.].

References

[1] A. Fire, S. Xu, M.K. Montgomery, S.A. Kostas, S.E. Driver, C.C. Mello, Potent and specific genetic interference by double-stranded RNA in *Caenorhabditis elegans*, Nature 391 (1998) 806–811.
[2] D.M. Dykxhoorn, C.D. Novina, P.A. Sharp, Killing the messenger: short RNAs that silence gene expression, Nat. Rev. Mol. Cell Biol. 4 (2003) 457–467.
[3] T. Tuschl, A. Borkhardt, Small interfering RNAs: a revolutionary tool for the analysis of gene function and gene therapy, Mol. Interv. 2 (2002) 158–167.
[4] P.J. Paddison, J.M. Silva, D.S. Conklin, M. Schlabach, M. Li, S. Aruleba, V. Balija, A. O'Shaughnessy, L. Gnoj, K. Scobie, K. Chang, T. Westbrook, M. Cleary, R. Sachidanandam, W.R. McCombie, S.J. Elledge, G.J. Hannon, A resource for large-scale RNA-interference-based screens in mammals, Nature 428 (2004) 427–431.
[5] Y. Dorsett, T. Tuschl, SiRNAs: applications in functional genomics and potential as therapeutics, Nat. Rev. Drug Discov. 3 (2004) 318–329.
[6] G.J. Hannon, J.J. Rossi, Unlocking the potential of the human genome with RNA interference, Nature 431 (2004) 371–378.
[7] E. Ashihara, E. Kawata, T. Maekawa, Future prospects of RNA interference for cancer therapies, Curr. Drug Targets, in press..
[8] L.J. Scherer, J.J. Rossi, Approaches for the sequence-specific knockdown of mRNA, Nat. Biotechnol. 21 (2003) 1457–1465.
[9] T. Holen, M. Amarzguioui, M.T. Wiiger, E. Babaie, H. Prydz, Positional effects of short interfering RNAs targeting the human coagulation trigger tissue factor, Nucleic Acids Res. 30 (2002) 1757–1766.
[10] Q. Du, H. Thonberg, J. Wang, C. Wahlestedt, Z. Liang, A systematic analysis of the silencing effects of an active siRNA at all single-nucleotide mismatched target sites, Nucleic Acids Res. 33 (2005) 1671–1677.
[11] D.S. Schwarz, H. Ding, L. Kennington, J.T. Moore, J. Schelter, J. Burchard, P.S. Linsley, N. Aronin, Z. Xu, P.D. Zamore, Designing siRNA that distinguish between genes that differ by a single nucleotide, PLoS Genet. 2 (2006) e140.
[12] A. Reynolds, D. Leake, Q. Boese, S. Scaringe, W.S. Marshall, A. Khvorova, Rational siRNA design for RNA interference, Nat. Biotechnol. 22 (2004) 326–330.
[13] M. Amarzguioui, H. Prydz, An algorithm for selection of functional siRNA sequences, Biochem. Biophys. Res. Commun. 316 (2004) 1050–1058.
[14] Y. Naito, T. Yamada, K. Ui-Tei, S. Morishita, K. Saigo, siDirect: highly effective, target-specific siRNA design software for mammalian RNA interference, Nucleic Acids Res. 32 (2004) W124–W129.
[15] K. Ui-Tei, Y. Naito, F. Takahashi, T. Haraguchi, H. Ohki-Hamazaki, A. Juni, R. Ueda, K. Saigo, Guidelines for the selection of highly effective siRNA sequences for mammalian and chick RNA interference, Nucleic Acids Res. 32 (2004) 936–948.
[16] W. Li, L. Cha, Predicting siRNA efficiency, Cell. Mol. Life Sci. 64 (2007) 1785–1792.
[17] P. de Felipe, Polycistronic viral vectors, Curr. Gene Ther. 2 (2002) 355–378.
[18] S.M. Ngoi, A.C. Chien, C.G. Lee, Exploiting internal ribosome entry sites in gene therapy vector design, Curr. Gene Ther. 4 (2004) 15–31.
[19] H. Hirai, P. Zhang, T. Dayaram, C.J. Hetherington, S. Mizuno, J. Imanishi, K. Akashi, D.G. Tenen, C/EBPbeta is required for 'emergency' granulopoiesis, Nat. Immunol. 7 (2006) 732–739.
[20] R. Kumar, D.S. Conklin, V. Mittal, High-throughput selection of effective RNAi probes for gene silencing, Genome Res. 13 (2003) 2333–2340.
[21] Q. Du, H. Thonberg, H.Y. Zhang, C. Wahlestedt, Z. Liang, Validating siRNA using a reporter made from synthetic DNA oligonucleotides, Biochem. Biophys. Res. Commun. 325 (2004) 243–249.
[22] N. Smart, P.J. Scambler, P.R. Riley, A rapid and sensitive assay for quantification of siRNA efficiency and specificity, Biol. Proced. Online 7 (2005) 1–7.

[23] C.F. Hung, K.C. Lu, T.L. Cheng, R.H. Wu, L.Y. Huang, C.F. Teng, W.T. Chang, A novel siRNA validation system for functional screening and identification of effective RNAi probes in mammalian cells, Biochem. Biophys. Res. Commun. 346 (2006) 707–720.
[24] H.Y. Ho, M.L. Cheng, Y.H. Wang, D.T. Chiu, Flow cytometry for assessment of the efficacy of siRNA, Cytometry A 69 (2006) 1054–1061.
[25] E. Martinez-Salas, Internal ribosome entry site biology and its use in expression vectors, Curr. Opin. Biotechnol. 10 (1999) 458–464.
[26] M. Stoneley, A.E. Willis, Cellular internal ribosome entry segments: structures, trans-acting factors and regulation of gene expression, Oncogene 23 (2004) 3200–3207.